Identification of Candidate Mitochondrial Inheritance Determinants Using the Mammalian Cell-Free System.

Dalen Zuidema[a], Alexis Jones[a], Won-Hee Song[a], Michal Zigo[a], Peter Sutovsky[a,b,*].

[a]Division of Animal Sciences, University of Missouri, Columbia, MO 65211-5300; [b]Department of Obstetrics, Gynecology and Women's Health, University of Missouri, Columbia, MO 65211-5300; *Correspodence: SutovskyP@missouri.edu.com; Tel.: +1-(573)-882-3329

Abstract: The degradation of sperm-borne mitochondria after fertilization is a conserved event. This process known as post-fertilization sperm mitophagy, ensures exclusively maternal inheritance of the mitochondria-harbored mitochondrial DNA genome. This mitochondrial degradation is in part carried out by the ubiquitin proteasome system. In mammals, ubiquitin-binding pro-autophagic receptors such as SQSTM1 and GABARAP have also been shown to contribute to sperm mitophagy. These systems work in concert to ensure the timely degradation of the sperm-borne mitochondria after fertilization. We hypothesize that other receptors, cofactors, and substrates are involved in post-fertilization mitophagy. Mass spectrometry was used in conjunction with a porcine cell-free system to identify other autophagic cofactors involved in post-fertilization sperm mitophagy. This porcine cell-free system is able to recapitulate early fertilization proteomic interactions. Altogether, 185 proteins were identified as statistically different between control and cell-free treated spermatozoa. Six of these proteins were further investigated, including MVP, PSMG2, PSMA3, FUNDC2, SAMM50, and BAG5. These proteins were phenotyped using porcine *in vitro* fertilization, cell imaging, proteomics, and the porcine cell-free system. The present data confirms the involvement of known mitophagy determinants in the regulation of mitochondrial inheritance and provides a master list of candidate mitophagy co-factors to validate in the future hypothesis-driven studies.

Introduction

Mitochondria are specialized cellular organelles which serve as the powerhouses of the cell. Mitochondria have been designated as such because of the large amounts of adenosine 5'-triphosphate (ATP) which they generate through both the TCA cycle as well as the electron transport chain. Additionally, mitochondria play roles in various cellular signaling pathways, serve as a calcium ion storage structure, help regulate cellular metabolism (McBride, Neuspiel, & Wasiak, 2006), and can signal for apoptosis (Hajnóczky et al., 2006). Mitochondria are also unique among cellular organelles because they house their own genome distinct from that of the nuclear DNA. This DNA is referred to as mitochondrial or mtDNA. The mtDNA encodes for 13 proteins which are used within the electron transport chain, as well as 22 tRNAs, and 2 rRNAs (Anderson et al., 1981). Mitochondria and the mtDNA which they harbor are almost exclusively inherited from the maternal lineage in most animal species, including humans. This pattern of maternal inheritance results in a single haplotype of the mtDNA being present in offspring.

This pattern of maternal inheritance results in most individual animals inheriting one mitochondrial genome from their mothers. Though naturally occurring maternally derived heteroplasmy (the presence of two distinct populations of mtDNA haplotypes) caused by mutations of the mitochondrial genome is observed (McFarland, Taylor, & Turnbull, 2007), heteroplasmy caused by the inheritance of the father's mtDNA is very rare (Luo et al., 2018; Schwartz & Vissing, 2002). Furthermore, in laboratory settings, researchers have been able to cause heteroplasmy in mice (Sharpley et al., 2012). These heteroplasmic mice were both mentally and physiologically insufficient when compared to their homoplasmic counterparts. The nematode roundworm *Caenorhabditis elegans* has also been utilized in this area of research. These worms were given a specific mtDNA deletion which caused the entire population to become heteroplasmic. It was found that embryonic lethality was 23-fold higher; they had reduced metabolic rates, and the males experienced reduced sperm mobility in this population of worms when compared to homoplasmic counterparts (Liau, Gonzalez-Serricchio, Deshommes, Chin, & LaMunyon, 2007). Thus, in both laboratory animal populations, heteroplasmy was shown to be detrimental. It has also been observed that this mtDNA maternal inheritance pattern has been naturally violated in some human offspring (Luo et al., 2018; Schwartz & Vissing, 2002; Slone et al., 2020). Several multigenerational families have been identified with various forms of paternal mtDNA leakage. In the case of these studies, the heteroplasmy was identified because one of the family members had a mitochondrial

disease. Though some of the relatives seemed to carry benign levels of paternal heteroplasmy, other family members were not so fortunate. Again, showing that when paternal mitochondria are not eliminated, it appears to eventually result in reduced health and fitness outcomes.

The paternal, sperm-borne mitochondria are located on the midpiece of the sperm tail, within a structure known as the mitochondrial sheath. This sheath organizes mitochondria into a compact helical configuration and in the livestock mammalian species, this sheath contains 50 to 75 mitochondria (Ankel-Simons & Cummins, 1996). This mitochondrial sheath structure is quickly degraded from the fertilizing spermatozoa upon entry into the oocyte cytoplasm in a process known as post-fertilization sperm mitophagy. This mitophagic process is a nuanced autophagic and proteasome-dependent degradation of the mitochondria. It has been shown that ubiquitin associates with the sperm mitochondria in primate, ruminant, and rodent oocyte cytoplasm (P. Sutovsky et al., 1999). It has also been demonstrated that the ubiquitination of sperm mitochondria takes place in the porcine zygote, where the effect of proteasomal inhibitors on sperm mitophagy was described for the first time and resulted in implicating the ubiquitin proteasome system as a pivotal part of this mitophagic process (Sutovsky, McCauley, Sutovsky, & Day, 2003; Sutovsky, Van Leyen, McCauley, Day, & Sutovsky, 2004). More recently, studies using *Caenorhabditis elegans* and *Drosophila* revisited the concept of ubiquitin-dependent post-fertilization sperm mitophagy, with a focus on the autophagic branch of this complex pathway (Al Rawi et al., 2011; Politi et al., 2014; Sato & Sato, 2011; Zhou, Li, & Xue, 2011). Much of the data from this research has focused on a handful of autophagic proteins. These proteins included sequestosome 1 (SQSTM1), GABA type A receptor-associated protein (GABARAP), microtubule-associated protein 1 light chain 3α (LC3), and valosin-containing protein (VCP). Further research has shown synergistic efforts between SQSTM1, GABARAP, and VCP in porcine sperm mitophagy (W. H. Song, Yi, Sutovsky, Meyers, & Sutovsky, 2016). To build upon this research, a better understanding of the potential co-factors, substrates, other proteins, and other pathways involved in post-fertilization sperm mitophagy is necessary.

The porcine cell-free system used in the present study is designed to recapitulate early fertilization proteomic interactions which would take place upon the incorporation of the spermatozoa into the ooplasm. It is a powerful tool that was used in this study (W. H. Song & Sutovsky, 2018), adapted from a similar amphibian system utilizing the eggs of an African clawed frog, *Xenopus laevis* (Miyamoto et al., 2007; Miyamoto et al., 2009; Sutovsky, Simerly, Hewitson, & Schatten, 1998). Our porcine system utilizes small porcine oocytes (100 µm diameter) matured *in vitro*, instead of very large, easy to harvest frog eggs (1.2 mm diameter). Compared to other mammalian models, porcine oocytes are relatively easy to collect and mature (to fertilization-ready metaphase II stage) in large quantities. Furthermore, the timing of post-fertilization sperm mitophagy in porcine zygotes is favorable as it occurs prior to the 1st embryo cleavage (Sutovsky et al., 2003); thus, this system can be utilized to study post-fertilization sperm mitophagy in a shorter time span and without interfering with the established role of the ubiquitin-proteasome system in cell division, a feat that would be more complicated in a bovine embryo where the post-fertilization sperm mitophagy occurs between the 2 and 4 cell stage (Peter Sutovsky et al., 1999). Furthermore, *Xenopus* egg extracts do not lend themselves to the study of mammalian sperm mitophagy as it is a species-specific recognition and degradation process. To prepare oocyte extracts for this system, MII oocytes are denuded of their cumulus cells and zona pellucida, then placed in an extraction buffer and subjected to three rounds of flash freezing followed by thawing to disrupt their cellular membranes. At that point, the oocytes are centrifuged at high speed to be crushed, and the supernatant present is collected. This oocyte extract contains cytoplasmic proteins and some of the lysosomal and autophagosomal membrane fractions that participate in mitophagy. The paternal component of this cell-free system is represented by boar spermatozoa primed through a demembranating treatment

with lysophosphatidylcholine (lysolecithin) followed by disulfide bond reduction via dithiothreitol (DTT), a stepwise treatment which removes the plasma and outer acrosomal membranes of the spermatozoa and destabilizes the structural sperm proteins in a fashion similar to sperm demembranation during sperm-oocyte fusion and disulfide bond reduction in the sperm head and tail at the time of sperm incorporation in the oocyte cytoplasm. Thus, this chemical demembranation and destabilization is used to replicate *in vivo* spermatozoa processing during natural fertilization. These primed spermatozoa are then co-incubated with the oocyte extract for 4 to 24 hours and early fertilization-specific proteomic interactions can be recapitulated. The porcine cell-free system allows us to observe thousands of spermatozoa interacting with ooplasmic proteins in a single trial, thus overcoming the limiting factor of one spermatozoon per fertilized egg, as seen in *in vitro* fertilization (IVF) and intracytoplasmic sperm injection (ICSI) protocols. This cell-free system has been previously shown to recapitulate fertilization sperm mitophagy events which take place in a zygote (W.-H. Song et al., 2021; W. H. Song & Sutovsky, 2018).

In this study, the porcine cell-free system was used in conjunction with MADLI-TOF mass spectrometry to conduct a quantitative investigation of early fertilization proteomics (**Fig. 1**). Two different trials were conducted each containing biological triplicates and based on this data an inventory of 185 proteins ($p<0.1$) of potential interest in the context of post-fertilization sperm mitophagy was compiled. Six of these proteins were further investigated, including major vault protein (MVP), proteasomal assembly chaperone 2 (PSMG2), proteasomal subunit alpha 3 (PSMA3), FUN14 domain-containing protein 2 (FUNDC2), sorting and assembly machinery component 50 (SAMM50), and BAG family molecular chaperone regulator 5 (BAG5). These six proteins were considered candidate mitophagy proteins of interest based on their known functions in established autophagy-related pathways. The investigation was an attempt to understand these proteins in more detail than what was extrapolated from the mass spectrometry data. We once again used the porcine cell-free system, but this time in conjunction with immunocytochemistry (ICC) and Western blotting (WB), to characterize the localization and modification changes these proteins underwent within the system. Furthermore, we investigated these proteins in zygotes after IVF to characterize their localization patterns during *in vitro* fertilization.

Results

Quantitative Proteomics with the Cell-Free System

MALDI-TOF mass spectrometry was used to analyze spermatozoa which were exposed to the porcine cell-free system. The goal of this mass spectrometry trial was to capture changes in protein quantities between control primed spermatozoa samples (no extract exposure) and cell-free system treated sperm samples. Vehicle control sperm samples were also submitted, as were samples of oocyte extract. A workflow diagram of the study is shown in **Figure 1**. Three biological replicates of this trial were submitted to compare primed control vs cell-free treated sperm after 4 hours of cell-free system co-incubation; separately, three biological replicates were submitted to compare primed control vs cell-free treated spermatozoa after 24 hours of cell-free system co-incubation. During both trials, 3 biological replicates of vehicle control sperm and oocyte extract were submitted as well. Raw data captured from mass spectrometry was referenced against the *Sus scrofa* UniProt Knowledge base, thus capturing an inventory of proteins present in each sample and their relative abundance. The samples were normalized based on the content of outer dense fiber protein 1, 2, and 3 and then subjected to statistical analysis. The primed control and cell-free treated sperm samples were statistically compared by using a paired T-test. This T-test compared the relative normalized protein abundance between the primed control and cell-free treated samples. A P-value of 0.2 (class 1), or 0.1 (class 2 and 3) was considered statistically relevant for the purpose of this study.

After T-test analysis in the 4-hour trial, 138 proteins were found to undergo changes ($p<0.1$) in abundance between the primed control vs. cell-free treated spermatozoa. In the 24-hour trial, 56 proteins were ($p<0.1$) different in abundance between the primed control and cell-free treated spermatozoa. Of these significant proteins from each trial, 14 overlapped, resulting in a total of 180 statistically different proteins identified between the two trials. Between the two trials, 24 proteins were only found in cell-free treated sperm samples and were not present in the primed control samples. These proteins were assumed to be proteins from the oocyte extract which remained bound to spermatozoa after extract co-incubation. For proteins that followed this pattern, we loosened our statistical parameters and included proteins in our inventory out to $p<0.2$. In the 4-hour trial, this resulted in 6 more proteins being included, and in the 24-hour trial, this resulted in 7 additional proteins. Of these 13 proteins, 8 overlapped; thus, this inclusion step added 5 more proteins to our inventory for a grand total of 185 proteins. The 4-hour inventory ultimately included 144 proteins of interest (**Table 1**), whereas the 24-hour inventory contained 63 proteins of interest (**Table 2**). These inventories had an overlap of 22 proteins. The full data sheets including all reps for the 4- and 24-hour trials as well as the normalizations and T-test analyses can be found in **Table S1**.

Both the 4-hour and 24-hour protein inventories were divided into three different classes. Class 1 proteins were detected only in the oocyte extract (absent in the vehicle control and primed control spermatozoa) and found on the spermatozoa only after extract co-incubation. These proteins are interpreted as ooplasmic mitophagy receptors/determinants and nuclear/centrosomal remodeling factors. Class 2 proteins were detected in the primed control spermatozoa but increased in the spermatozoa exposed to cell-free system co-incubation. Class 3 proteins were present in both the gametes or only the primed control spermatozoa, but are decreased in the spermatozoa after co-incubation, interpreted as sperm borne mitophagy determinants and/or sperm-borne proteolytic substrates of the oocyte autophagic system. These protein inventories, sorted by class for both the 4- and 24-hour trials, can be found in **Tables 1** and **2**, respectively.

The functions of all the proteins added to these inventories were manually searched and categorized by using the UniProt Knowledgebase as well as PubMed literature search. Based on known functions, all proteins were categorized, and pie charts were rendered (**Figure 2A-F**). It should be noted that our Mass Spectrometry generated data was analyzed for proteins by using the UniProt Knowledgebase and was only analyzed for known *Sus scrofa* proteins.

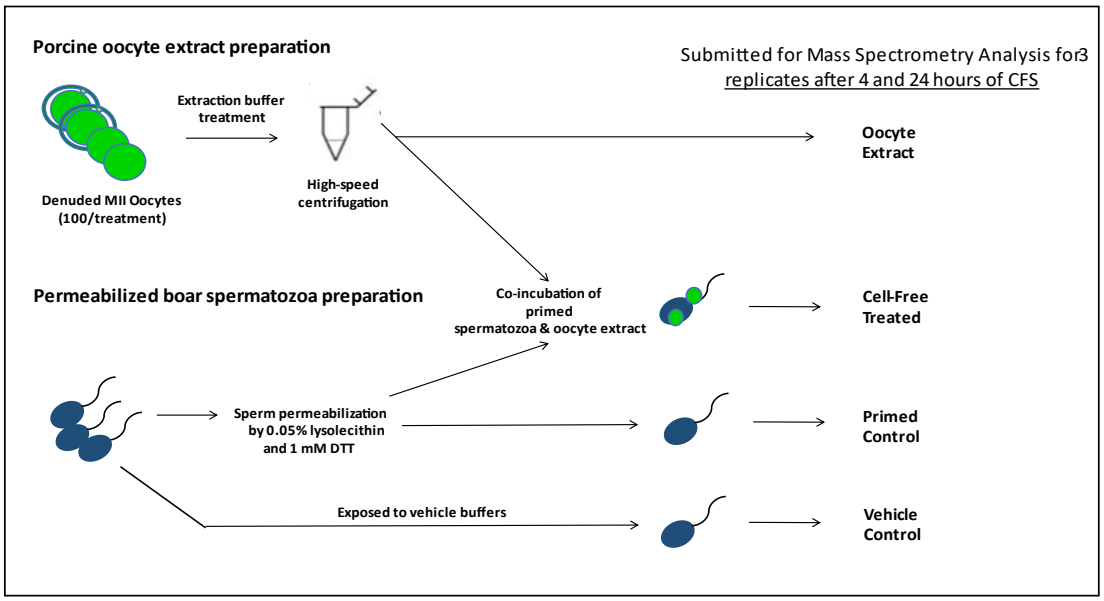

Figure 1. The porcine cell-free system and workflow diagram for the preparation of samples for mass spectrometry analysis.

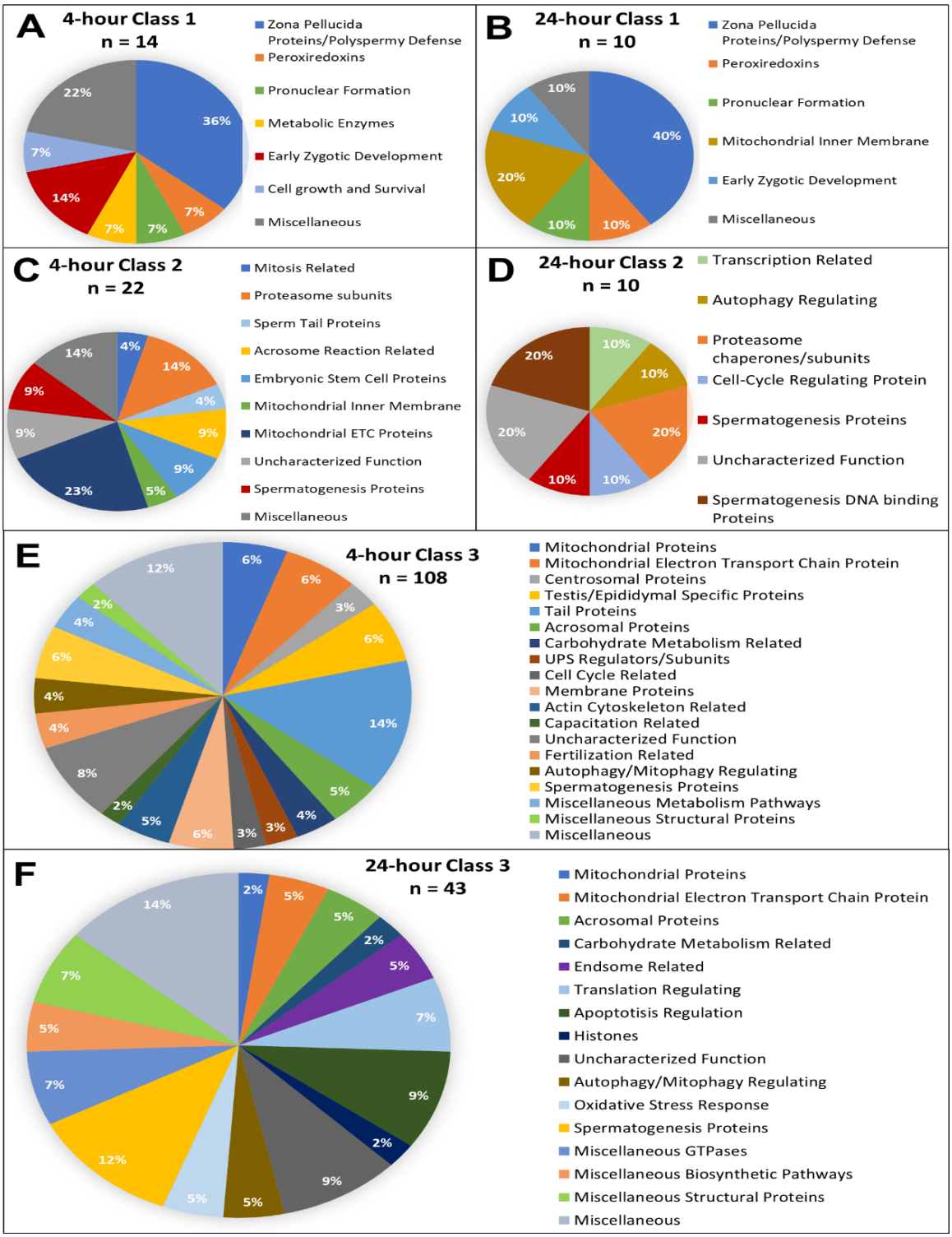

Figure 2. Candidate protein categorization by their functions. Proteins found in different amounts after cell-free system coincubation at both 4 and 24 hours are categorized by function as found on Uniprot.org and literature via Pubmed.com. Protein characterizations of Class 1 found only in cell-free treated spermatozoa samples after 4 hours of cell-free system co-incubation (**A**), and 24 hours of cell-free system co-incubation (**B**) vs primed control spermatozoa ($p<0.2$). Characterization of Class 2 proteins which underwent an increase in abundance ($p<0.1$) in cell-free treated spermatozoa during the 4-hour (**C**) and 24-hour (**D**) cell-free system trials vs primed control spermatozoa. Class 3 proteins, which underwent a decrease in abundance ($p<0.1$) in cell-free treated spermatozoa after 4 hours (**E**) and 24 hours (**F**) of cell-free system co-incubation vs primed control spermatozoa.

207
208 **TABLE 1:** Proteomic identification of mitophagy and sperm remodeling cofactors in the porcine cell-free system after 4 hours of co-
209 incubation.

Protein of Interest Legend: GN = Gene name PE = protein existence level SV = Sequence version (PE and SV only included for proteins which had multiple versions in the table)	Proposed role in autophagy/mitophagy/post-fertilization sperm structure remodeling by zygote, and original references describing identified proteins' role in those events.	P value based on 3 rep T-test analysis
CLASS 1 – Proteins detectable on spermatozoa only after extract exposure.		
Metalloendopeptidase a.k.a. Ovastacin GN: ASTL	Member of peptidase family involved in reproductive protein processing in *Drosophila;* (ov)astacin is secreted by mouse oocyte to cleave zona, prevent polyspermy. Ram *et al.,* 2006 DOI: 10.1073/pnas.0606228103 ; Burkart *et al.,* 2012; DOI: 10.1083/jcb.201112094	0.00003
Zona pellucida sperm-binding protein 3 GN: ZP3 (PE: 1, SV: 1)	Involved in sperm-egg recognition, acrosomal reaction, and polyspermy defense. Zimmerman *et al.,* 2011 DOI: 10.1371/journal.pone.0017256	0.00003
Major vault protein GN: MVP	Regulates cell growth and survival through the STAT3 and Akt signaling pathways. Das *et al.,* 2016 DOI: 10.1016/j.cellsig.2015.10.007	0.00006
Peptidyl arginine deiminase 6 GN: PADI6	Essential for early zygotal development, specifically cytoskeletal sheet formation through citrullination. Essential for female fertility. Esposito *et al.,* 2007 DOI: 10.1016/j.mce.2007.05.005	0.00007
Malic enzyme GN: ME2	Participates in pyruvate metabolic process, located in the mitochondria. www.unitprot.org	0.00008
Aprotinin Accession: B0LXF7	A serine protease inhibitor which decreases bleeding. Robert *et al.,* 1996 DOI: 10.1177/106002809603000410	0.0001
Zona pellucida sperm-binding protein 4 GN: ZP4	Involved in sperm-egg recognition, acrosomal reaction, and polyspermy defense. Zimmerman *et al.,* 2011 DOI: 10.1371/journal.pone.0017256	0.0002
Uncharacterized protein GN: PRDX3	Necessary for normal mitochondrial function. Localizes to the mitochondria after peroxide exposure and acts as a peroxide reducing agent. Wonsey *et al.,* 2002 DOI: 10.1073/pnas.102523299	0.0006
Zona pellucida sperm-binding protein 3 GN: ZP3 (PE: 4, SV: 1)	Involved in sperm-egg recognition, acrosomal reaction, and polyspermy defense. Zimmerman *et al.,* 2011 DOI: 10.1371/journal.pone.0017256	0.1835
DNA (cytosine-5)-methyltransferase GN: DNMT1	Helps maintain DNA methylation problems through cell divisions. It is found within the cytoplasm of MII oocytes and early-stage embryos, later localizing to the nuclei of 8 – 16 cell embryos. Lodde *et al.,* 2009 DOI: 10.4081/ejh.2009.e24	0.1835
Nucleophosmin/nucleoplasmin 2 GN: NPM2	Sperm nucleus remodeling after fertilization. Required for histone import into paternal pronucleus. McLay & Clark., 2003 DOI: 10.1530/rep.0.1250625	0.1836
Zona pellucida sperm-binding protein 2 GN: ZP2 (SV:2)	Involved in sperm-egg recognition, acrosomal reaction, and polyspermy defense. Zimmerman *et al.,* 2011 DOI: 10.1371/journal.pone.0017256	0.1837
1-aminocyclopropane-1-carboxylate synthase homolog (inactive) like GN: ACCSL	Binds pyridoxal phosphates and has catalytic activity. www.uniprot.org	0.1842
Extended synaptotagmin 1 GN: ESYT1	Located in the ER and acts as a lipid transport protein. Interacts with PI(4,5)P, and calcium to transfer lipids through membranes. Xie *et al.,* 2018 DOI: 10.1096/fj.201801878R	0.1859
CLASS 2 - Detected in the vehicle and primed control spermatozoa, increased in extract-exposed spermatozoa.		

Peroxiredoxin 2 GN: PRDX2 (SV: 1)	Antioxidant enzyme that plays role in ROS protection immediately after fertilization. Morita *et al.,* 2018 DOI: 10.1262/jrd.2018-005	0.0004
Cytochrome c1 GN: CYC1	Part of the mitochondrial electron transport chain. Forms a complex with cytochrome c and cytochrome oxidase. Located on the inner mitochondrial membrane. Chiang & King 1979 PMID:33986	0.0125
Cytochrome c oxidase subunit 5A GN: COX5A	Cytochrome c oxidase is a protein complex made up of 13 subunits encoded by mtDNA and nuclear DNA. Without COX5A, cytochrome c oxidase fails to form. Fornuskova *et al.,* 2010 DOI: 10.1042/BJ20091714	0.0143
Proteasome subunit alpha type: PSMA3 & PSMA2	Pharmacological inhibition of 20S core activity prevents sperm mitophagy in porcine zygote. Sutovsky *et al.,* 2003 DOI: 10.1095/biolreprod.102.012799	0.0152
Stomatin like 2 GN: STOML2	Mitochondrial protein which forms microdomains within the inner membrane. It is a regulator of mitochondrial translation. Mitsopoulos *et al.,* 2017 DOI: 10.1371/journal.pone.0179967	0.0174
Outer dense fiber of sperm tails 2 GN: ODF2	Sperm flagellum and centrosomal protein. Play a critical role in embryo preimplantation, this role remains unknown. Salmon *et al.,* 2006 DOI: 10.1002/dvg.20241	0.0199
Uncharacterized protein GN: NDUFB5	Part of the mitochondrial respiratory chain complex I assembly. Integral component of the mitochondrial inner membrane. www.uniprot.org	0.0219
A-kinase anchoring protein 4 GN: AKAP4	Flagellated sperm motility, transmembrane receptor protein serine/threonine kinase signaling pathway, located in the sperm principal piece. Assists in capacitation and acrosome reaction. Ben-Navi *et al.,* 2016 DOI: 10.1038/srep37922	0.0424
RIB43A domain with coiled-coils 1 GN: RIBC1	A protein which is overexpressed in high fertility bull sperm. However, its function is not known. Muhammad Aslam *et al.,* 2018 DOI: 10.1016/j.theriogenology.2018.06.021	0.0438
NADH:ubiquinone oxidoreductase subunit B9 GN: NDUFB9	Part of the mitochondrial respiratory chain complexes, specifically Complex I. Mutations of this subunit cause CI deficiency. One of the subunits responsible for CI and CIII interactions. Wu *et al.,* 2016 DOI: 10.1016/j.cell.2016.11.012	0.0465
Uncharacterized protein Accession: A0A287A4B9	BPTI/Kunitz inhibitor domain-containing protein. Serine-type endopeptidase inhibitor activity. Gene name: PTI. www.uniprot.org	0.049
Testis-specific serine kinase 6 GN: TSSK6	Involved in sperm chromatin condensation, and crucial for spermiogenesis. Heat shock protein 90 regulates TSSK6 and shields it from ubiquitin-mediated catabolism. Jha *et al.,* 2013 DOI: 10.1074/jbc.M112.400978	0.0497
Uncharacterized protein GN: OAZ3	OA3 is expressed specifically during spermiogenesis. Essential for rigid junction between the head and tail of spermatozoa. Tokuhiro *et al.,* 2009 DOI: 10.1371/journal.pgen.1000712	0.0615
NADH:ubiquinone oxidoreductase subunit B10 GN: NDUFB10	Part of the mitochondrial respiratory chain complexes, specifically Complex I. One of the subunits which forms intramolecular disulfides within CI. Wu *et al.,* 2016 DOI: 10.1016/j.cell.2016.11.012	0.0694
Chromosome 9 open reading frame 135 GN: C9orf135	Down regulated during gametogenesis. Believed to encode a membrane protein which serves as a surface marker for undifferentiated embryonic stem cells. Zhou *et al.,* 2017 DOI: 10.1038/srep45311	0.0705

Tektin 2 GN: TEKT2	Associates with and organizes the central spindle during mitosis. Durcan *et al.,* 2008 DOI: 10.1083/jcb.200711160	0.0736
Uncharacterized protein GN: BANF1	Contributes to embryonic stem cell self-renewal properties, preventing them from differentiating too quickly. Cox *et al.,* 2011 DOI: 10.1242/jcs.083238	0.0771
Chromosome 4 open reading frame 45 GN: C4orf45	Uncharacterized function. www.uniprot.org	0.0914
Proteasome subunit alpha type GN: PSMA8	A testis specific proteasomal subunit found during spermatogenesis. Appears crucial for proper meiotic exit by the forming spermatids. Gomez-H *et al.,* 2019 DOI: 10.1371/journal.pgen.1008316	0.092
Tektin 1 GN: TEKT1	Found in both the acrosome and flagella of spermatozoa. May participate in sperm head cytoskeletal roles or serve a function in the acrosome reaction. Oiki *et al,* 2014 DOI: 10.2108/zsj.31.101	0.0922
Ferritin GN: FTH1	Acts as an inhibitor of death domain-associated protein (Daxx), which serves as an inhibition of the Daxx apoptosis pathway. Liu *et al.,* 2012 DOI: 10.1007/s11033-011-0811-5	0.0949
CLASS 3 - Detected in spermatozoa before extract exposure, reduced after extract exposure.		
Oxoglutarate dehydrogenase like GN: OGDHL	A rate limiting component of the OGDH complex, a mitochondrial protein complex. OGDHL regulates cell growth, apoptosis and seems to play a role in cancer development when overexpressed. Sen *et al.,* 2012 DOI: 10.1371/journal.pone.0048770	0.0008
Kinesin-like protein GN: KIF5B	Involved in centrosome localization, cytoplasmic organization and assists with regulating protein localization to the plasma membrane. www.uniprot.org	0.0008
Dpy-19 like 2 GN: DPY19L2	Proposed to serve as an anchor between the acrosome and the nucleus of the sperm. It is required for proper acrosome spreading and head formation during spermatogenesis. Pereira *et al.,* 2019 DOI: 10.1111/brv.12498	0.0021
Coiled-coil domain containing 188 GN: CCDC188	Identified as a novel candidate gene for retinitis pigmentosa. However, function remains unknown. Yi *et al.,* 2020 DOI: 10.1016/j.ebiom.2020.102792	0.0033
Uncharacterized protein GN: LOC110255463	Glyco_hydro_35 domain-containing protein. Beta-galactosidase activity within the carbohydrate metabolic pathway. www.uniprot.org	0.0034
Leucine zipper transcription factor like 1 GN: LZTFL1	Interacts with Bardet-Biedl Syndrome protein complex and regulates this complex's ciliary traffic and signaling. Seo *et al.,* 2011 DOI: 10.1371/journal.pgen.1002358	0.0034
Peptidyl-prolyl cis-trans isomerase GN: PPIL1	Participates in mRNA splicing, protein folding and peptidyl-prolyl isomerization. www.uniprot.org	0.0037
NmrA like redox sensor 1 GN: NMRAL1	Transcriptional regulator which responds to cell metabolism by causing changes in gene expression. Garciandia & Suarez 2013 DOI: 10.1016/j.ydbio.2013.06.013	0.0042
Glycogen synthase kinase 3 beta variant 5 GN: GSK3B	Mediates the phosphorylation of MCL1. Once phosphorylated, MCL1 undergoes ubiquitination and proteasomal degradation which releases BECLIN1 to induces axonal autophagy. Wakatsuki *et al.,* 2017 DOI: 10.1083/jcb.201606020	0.0048
mRNA export factor GN: RAE1	Active during interphase as a mitotic checkpoint and spindle assembly regulator. When inhibited, defects in spindle organization, chromosome alignment and segregation, and delayed cell cycle progression were observed. Lee *et al.,* 2009 DOI: 10.1111/j.1365-313X.2009.03869.x	0.0048

Cullin 4B GN: CUL4B	E3 ubiquitin ligase believed to initiate polyubiquitination of y-tubulin and thereby control centrosomal stability through ubiquitination of y-tubulin. Thirunavukarasou *et al,* 2015 DOI: 10.1007/s11010-014-2309-7	0.0049
Uncharacterized protein Accession: F1RHJ8	No described function www.uniprot.org	0.0053
Dihydroxyacetone phosphate acyltransferase GN: GNPAT	Part of the plasmalogen biosynthetic pathway. Plasmalogens make up the spermatozoa membrane and play a role in their maturation. Reisse *et al.,* 2001 DOI: 10.1095/biolreprod64.6.1689	0.0058
26S proteasome non-ATPase regulatory subunit 2 GN: PSMD2	Necessary for cell proliferation and cell cycle progression. Interacts with p21 and p27 and mediates their ubiquitin-proteasomal degradation. Li *et al.,* 2018 DOI: 10.1016/j.canlet.2018.05.018	0.0083
Glutamine rich 2 GN: QRICH2	Necessary for proper sperm flagellum formation. Shen *et al.,* 2019 DOI: 10.1038/s41467-018-08182-x	0.0084
Sperm acrosome membrane-associated protein 1 GN: SPACA1	Involved in acrosome assembly, localized to the equatorial segment. Functions in sperm-egg fusion. Fujihara *et al.,* 2012 DOI: 10.1242/dev.081778	0.0087
cAMP-dependent protein kinase type I-alpha regulatory subunit GN: PRKAR1A	Interacts with A-kinase anchoring proteins and responds to intracellular cAMP concentrations. Barradeau *et al.,* 2002 DOI: 10.1016/s1050-1738(02)00167-6	0.0106
NADH dehydrogenase (ubiquinone) flavoprotein 1 mitochondrial GN: NDUFV1	Mitochondrial protein that is part of the electron transport chain. Part of complex I. Varghese *et al.,* 2015 DOI: 10.1093/hmg/ddv344	0.0107
Spermatogenesis associated 3 GN: SPATA3	Testis specific protein. Current function is unknown but believed important for spermatogenesis. Zhou *et al.,* 2020 DOI: 10.1007/s11033-019-04825-4	0.012
Actin like 7B GN: ACTL7B	A spermatogenesis-specific actin like protein. Tanaka *et al.,* 2019 DOI: 10.22074/ijfs.2019.5702	0.0121
Cytochrome c oxidase subunit 7A2 like GN: COX7A2L	Mitochondrial respiratory chain protein. Acts as a regulatory checkpoint for Complex III, however, is nonessential for mitochondrial respiration. Lobo-Jarne *et al.,* 2018 DOI: 10.1016/j.celrep.2018.10.058	0.0123
Triosephosphate isomerase GN: TPI1	Enzyme utilized during glycolysis. Catalyzes the conversion of DHAP to G3P. However, there is evidence suggesting that this is the same protein as P36, a sperm protein present along the acrosomal membrane and believed essential for normal fertilization. Auer *et al.,* 2004 DOI: 10.1002/mrd.20107	0.0126
Cilia and flagella associated protein 52 GN: CFAP52	Involved in the motility of flagella. www.uniprot.org	0.014
SUMO peptidase family member NEDD8 specific GN: SENP8	Contributes to proper cell cycle progression, and maintenance of neddylation levels. Coleman *et al.,* 2017 DOI: 10.7554/eLife.24325	0.0141
Fibrous sheath interacting protein 2 GN: FSIP2	Tail protein responsible for proper flagellum morphology. Martinez *et al.,* 2018 DOI: 10.1093/humrep/dey264	0.0144
Testis specific serine kinase 4 GN: TSSK4	Induces apoptosis in spermatogonia and spermatocytes. Seemingly functions as a quality assurance regulator of spermatogenesis. Wang *et al.,* 2015 DOI: 10.1007/s11596-015-1417-2	0.0146
Uncharacterized protein GN: LOC100626097	No described functions www.uniprot.org	0.0163
Serpin family B member 6 GN: SERPINB6	Serine protease inhibitor which is expressed in male germ cells and female somatic cells. Believed to play some role in gonad development, gametogenesis, and/or fertilization. Charron *et al,* 2006 DOI: 10.1002/mrd.20385	0.0164

Lon protease homolog mitochondrial GN: LONP1	A mitochondrial protease which participates in maturation of a subset of proteins which is necessary for mitochondrial proteostasis and normal gene expression. Rendon & Shoubridge 2018 DOI: 10.1128/MCB.00412-17	0.017
Vacuolar protein sorting 13 homolog A GN: VPS13A	Required for lipid transfer to various organelles, including the mitochondria, where it influences morphology. Yeshaw *et al.,* 2019 DOI: 10.7554/eLife.43561	0.018
Protein kinase cAMP-dependent type I regulatory subunit beta GN: PRKAR1B	Inhibits cAMP-dependent protein kinase pathways and binds the catalytic subunit of PKA www.uniprot.org	0.0189
Nardilysin convertase GN: NRD1_tv2	Metalloendopeptidase activity. Involved in protein catabolism and regulation of membrane ectodomain proteolysis. www.uniprot.org	0.0195
Creatine kinase B-type GN: CKB	Part of the phosphocreatine biosynthetic pathway. Binds ATP and produces N-phosphocreatine. www.uniprot.org	0.0195
Uncharacterized protein GN: LOC102158372	Integral membrane component. www.uniprot.org	0.0203
Protein phosphatase 1 regulatory subunit 9B GN: PPP1R9B	Involved in cell migration, calcium-mediated signaling and actin filament organization. www.uniprot.org	0.0205
Glutamine synthetase GN: GLUL	Enzyme which catalyzes the condensation of glutamate and ammonia to form glutamine. Cellular localization is regulated by GABA type B receptors. Huyghe *et al.,* 2014 DOI: 10.1074/jbc.M114.583534	0.0208
BAG family molecular chaperone regulator 5 isoform b GN: BAG5_tv3	Negatively regulates mitophagy through the suppression of Parkin recruitment. Snoo *et al.,* 2019 DOI: 10.1038/s41419-019-2132-x	0.0212
Lysozyme like 4 GN: LYZL4	Found in high levels in the acrosome and principal piece on spermatozoa. Shown to be important for fertilization. Sun *et al.,* 2011 DOI: 10.1093/abbs/gmr017	0.0226
Actin related protein T3 GN: ACTRT3	Found within male germ cell nuclei, part of the actin cytoskeleton. www.uniprot.org	0.0228
Phosphoglycerate kinase GN: PGK2	This enzyme is specific to sperm glycolysis and replaces the PGK1 enzyme found in all other cell types. Essential for sperm motility and ATP generation. Danshina et al., 2010 DOI: 10.1095/biolreprod.109.079699	0.0233
Protein interacting with cyclin A1 GN: PROCA1	Part of the phospholipid metabolic pathway. www.uniprot.org	0.0263
Dynein axonemal heavy chain 3 GN: DNAH3	Known to affect sperm motility & play a role in male fertility. Rezende *et al,* 2018 DOI: 10.1111/age.12710	0.0265
Epididymis-specific alpha-mannosidase GN: MAN2B2	Lysosomal type D-mannosidase found exclusively in epididymal fluid and sperm cells. Zhao *et al.,* 2019 DOI: 10.1016/j.theriogenology.2019.08.006	0.0284
Aldehyde dehydrogenase 1 family member A1 GN: ALDH1A1	Part of the retinoic acid signaling pathway in the testes. Plays a role in spermatogenesis and responds to gonadotropin stimulation. Nourashrafeddin & Rashidi 2018 PMID: 29436793	0.029
Translocase of outer mitochondrial membrane 34 GN: TOMM34	A chaperone-like protein which imports preproteins into the mitochondria. Blesa *et al,* 2008 DOI: 10.1139/o07-151	0.0306
Kinetochore localized astrin (SPAG5) binding protein GN: KNSTRN	Involved in chromosome segregation, regulation of attachment of spindle microtubules to kinetochore, & spindle organization. www.uniprot.org	0.033

Testin GN: TES	A protein which is secreted by Sertoli cells and regulates the blood-testis barrier. Also found in ovaries. Su *et al.,* 2020 DOI: 10.1002/jcp.29541	0.0332
Family with sequence similarity 170 member A GN: FAM170A	No described function. www.uniprot.org	0.0804
SAMM50 sorting and assembly machinery component GN: SAMM50	Regulator of PINK1-Parkin mediated mitophagy. A Samm50 depletion results in PINK1 build up, Parkin recruitment and subsequent mitophagy. Jian *et al.,* 2018 DOI: 10.1016/j.celrep.2018.05.015	0.0345
Fascin GN: FSCN3	Essential for spermatid development, establishment and maintenance of cell polarity, actin filament binding. Expressed in the spermatid head. Tubb *et al.,* 2002 DOI: 10.1006/excr.2002.5486	0.0347
Tyrosine 3-monooxygenase/tryptophan 5-monooxygenase activation protein zeta	Newly described regulator of capacitation-associated tyrosine phosphorylation. Saez *et al.,* 2019 DOI: 10.1111/andr.12634	0.0379
NSF attachment protein alpha GN: NAPA	Soluble N-ethylmaleimide-sensitive factor attaching activities. www.uniprot.org	0.0384
WD repeat domain 63 GN: WDR63	Upregulated by p53, negatively regulates cell migration, invasion, and metastasis. Zhao *et al,* 2020 DOI: 10.15252/embr.201949269	0.0422
Uncharacterized protein GN: LOC100154312	Involved with the centrosomes, but no described function. www.uniprot.org	0.0429
Zona pellucida-binding protein 1 GN: ZPBP	Important for acrosome assembly, as well as binding of sperm to the zona pellucida. Yatsenko *et al.,* 2012 DOI: 10.1093/molehr/gar057	0.043
Mitochondrial associated cysteine-rich protein GN: SMCP	Localized to the mitochondrial capsule and contributes to flagellum movement. Hawthorne *et al.,* 2006 DOI: 10.1016/j.ygeno.2005.09.010	0.0436
Uncharacterized protein GN: SCO2	Induces p53-mediated apoptosis. It is a cytochrome c oxidase assembly factor and increases reactive oxygen species production. Madan *et al.,* 2013 DOI: 10.1128/MCB.06798-11	0.0438
Epididymal sperm-binding protein 1 GN: ELSPBP1	In bovine, this protein binds dead sperm within the epididymis. D'Amours *et al.* 2012 DOI: 10.1095/biolreprod.112.100990;	0.0445
Armadillo repeat containing 4 GN: ARMC4	Participates in cilium movement and outer dynein arm assembly. www.uniprot.org	0.0448
Chromosome 1 open reading frame 56 GN: C1orf56	Regulates cell population proliferation. www.uniprot.org	0.0457
Regulator of G protein signaling 22 GN: RGS22	Regulates G-protein signaling during spermiogenesis. Hu *et al.,* 2008 DOI: 10.1095/biolreprod.107.067504	0.0457
Hypoxanthine-guanine phosphoribosyltransferase GN: HPRT1	Plays a role in purine regulation and generation through the salvage of IMP and GMP. Appears to be found in high amounts within many types of cancer cells Townsend *et al.,* 2018. DOI: 10.1007/s12032-018-1144-1	0.0468
Kinesin-like protein GN: KIF9	Testis specific kinesin. Regulates flagellar motility and acts as a molecular motor in spermatozoa tails. Miyata *et al.,* 2020 DOI: 10.1096/fj.201902755R	0.0468
Immunity-related GTPase family cinema protein GN: IRGC	GTPase activity, located in the cell membrane. www.uniprot.org	0.0476

Dynein axonemal heavy chain 17 GN: DNAH17	Sperm-specific axonemal outer dynein arm protein. Necessary for male fertility and normal flagellum movement and morphology. Whitfield *et al.,* 2019 DOI: 10.1016/j.ajhg.2019.04.015	0.0478
Vaccinia related kinase 3 GN: VRK3	Part of the Wnt signaling pathway, negatively regulates ERK1 & 2, and positively regulates phosphoprotein phosphatase activity. www.uniprot.org	0.0488
Dynein axonemal heavy chain 8 GN: DNAH8	Sperm-specific axonemal outer dynein arm protein. Necessary for male fertility and normal flagellum movement and morphology. Whitfield *et al.,* 2019 DOI: 10.1016/j.ajhg.2019.04.015	0.0498
Retinoic acid receptor responder 1 GN: RARRES1	Metalloendopeptidase inhibitor activity, found in the extracellular matrix. www.uniprot.org	0.0505
NADH:ubiquinone oxidoreductase subunit A9 GN: NDUFA9	Subunit required for complex I assembly in the electron transport chain. Mitochondrial protein. Baertling *et al.,* 2018 DOI: 10.1111/cge.13089	0.051
SEC13 homolog nuclear pore and COPII coat complex component GN: SEC13	Involved in COPII-coated vesicle budding and protein transport from the ER. www.uniprot.org	0.0512
Uncharacterized protein GN: LOC100514982	No described function www.uniprot.org	0.0514
L-lactate dehydrogenase C GN: LDHC	Testis specific isozyme found in male germ cells. Localizes to the principal piece in mature sperm but found in all spermatogenic cells. Appears to be required for fertilization. Goldberg *et al.,* 2010 DOI: 10.2164/jandrol.109.008367	0.0523
TBC1 domain family member 21 GN: TBC1D21	Localized to elongating spermatids during spermatogenesis, this protein appears to bind Rap1 (a protein crucial for proper spermatogenesis). Ke *et al.,* 2018 DOI: 10.3390/ijms19113292	0.0567
Uncharacterized protein GN: LOC100515166	IF rod domain-containing protein. Structural protein, part of the intermediate filaments. www.uniprot.org	0.0594
Uncharacterized protein GN: LOC100522130	Hydrolase activity utilizes magnesium as a cofactor. www.uniprot.org	0.0636
Actin like 9 GN: ACTL9	Part of the actin-based cytoskeleton. www.uniprot.org	0.065
NADH dehydrogenase (ubiquinone) iron-sulfur protein 6 mitochondrial GN: NDUFS6	Subunit of Complex I in the electron transport chain. Mitochondrial protein necessary for normal Complex I assembly. Kirby *et al,* 2004 DOI: 10.1172/JCI20683	0.0655
Uncharacterized protein GN: LOC102164346	FAM75 domain-containing protein. No characterized functions. www.uniprot.org	0.0665
Schlafen like 1 GN: SLFNL1	Testis-abundant protein. Shown to not be essential for male fertility. Park *et al,* 2020 DOI: 10.1093/biolre/ioaa084	0.0679
Dynein regulatory complex subunit 7 GN: DRC7	Required for flagellum formation and male fertility. Morohoshi *et al.,* 2020 DOI: 10.1371/journal.pgen.1008585	0.0693
Uncharacterized protein GN: PSMC2	Proteasome 26S subunit ATPase 2. Positively regulates RNA polymerase II complex assembly and participates in ubiquitin-dependent protein catabolism. www.uniprot.org	0.0694
Uncharacterized protein GN: PDHB	Pyruvate dehydrogenase B. Part of the pyruvate to acetyl-CoA pathway. www.uniprot.org	0.0701
Coiled-coil-helix-coiled-coil-helix domain containing 5 GN: CHCHD5	No characterized function. www.uniprot.org	0.0707

Actin related protein T2 GN: ACTRT2	Located in the post-acrosomal region and mid-piece of the sperm. Declines of this protein reduce sperm motility. Liu *et al,* 2015 DOI: 10.1111/andr.289	0.0714
Keratin 4 GN: KRT4	Part of the keratin filament-based components of the cytoskeleton. www.uniprot.org	0.0714
Ubiquitin thioesterase a.k.a. OTU deubiquitinase GN: OTUB1	Known deubiquitinating enzyme. Shown to regulate p53 and promote mitochondria-mediated apoptosis. Chen *et al.,* 2017 DOI: 10.18632/oncotarget.14278	0.0716
Rhophilin associated tail protein 1 like GN: ROPN1L	Sperm tail protein necessary for normal tail morphology and motility in sperm. Rattanachan *et al.,* 2014 DOI: 10.1016/j.actatropica.2014.08.002	0.0716
HYDIN axonemal central pair apparatus protein GN: HYDIN	Ciliary protein associated with heart tissue. Involved in GATA4 expression within heart tissues. Cao *et al.,* 2020 DOI: 10.1016/j.mod.2020.103611	0.0725
Heat shock 70 kDa protein 1-like GN: HSPA1L	Chaperone to HSP70 and found on the sperm plasma membrane. Naaby-Hansen & Herr 2010 DOI: 10.1016/j.jri.2009.09.006	0.0727
Actin like 7A GN: ACTL7A	A spermatogenesis-specific actin like protein. Tanaka *et al.,* 2019 DOI: 10.22074/ijfs.2019.5702	0.0729
T-complex protein 1 subunit gamma GN: CCT3	The t-complex protein 1 is a complex within cells which is responsible for protein folding. It is made up of 8 distinct subunits. Believed to interact with Zona-binding protein 2 and participate in sperm-zona binding. Dun *et al.,* 2011 DOI: 10.1074/jbc.M110.188888	0.0302
Uncharacterized protein Accession: A0A287AEH4	DUF4599 domain-containing protein. Membrane component protein. www.uniprot.org	0.0759
Phosphatidylethanolamine-binding protein 4 GN: pebp4	A secreted protein, unlike pebp1, 2, & 3. Inhibits ERK from activating EGF. Believed to participate in other pathways as well. He *et al,* 2016 DOI: 10.1016/j.bbamcr.2016.03.022	0.0764
Acyl-CoA synthetase long chain family member 6 GN: ACSL6	Required form normal spermatogenesis in mice. Highly expressed in spermatids. Shishikura *et al.,*2019 DOI: 10.1096/fj.201901074R	0.0774
NADH-cytochrome b5 reductase GN: CYB5R1	Flavoprotein involved in transferring reducing equivalents from NADH using FAD. Elahian *et al,* 2012 DOI: 10.3109/07388551.2012.732031	0.0802
Calmodulin 2	Calcium-mediated signaling & calcium ion binder. In stallion sperm, calmodulin plays a role in regulating sperm motility. Lasko *et al.,* 2012 DOI: 10.1016/j.anireprosci.2012.05.007	0.0804
Dynein axonemal heavy chain 7 GN: DNAH7	Involved in inner dynein arm assembly and cilium movement. www.uniprot.org	0.084
NADH dehydrogenase (ubiquinone) 1 subunit C2 GN: NDUFC2	Needed for proper mitochondrial function. Part of complex I in the electron transport chain of the mitochondria. Raffa *et al.,* 2019 DOI: 10.1016/j.ijcard.2019.02.027	0.0842
FUN14 domain-containing protein 2 GN: FUNDC2	FUNDC2 binds PIP3 and works through the AKT1/BAD/ BCL2L1 axis on the mitochondrial outer membrane. BCL2L1 protects cells against apoptotic hypoxia stress. A removal of FUNDC2 would coincide with a loss of stress protection and an increase in apoptosis and possibly mitophagy. Ma *et al.,* 2018 DOI: 10.1038/s41418-018-0121-8	0.0845
Dynein axonemal intermediate chain 2 GN: DNAI2	Plays a role in cilium movement, & outer dynein arm assembly. www.uniprot.org	0.0884

A-kinase anchoring protein 3 GN: AKAP3	Essential for sperm motility, capacitation, and the acrosome reaction. Degraded by tyrosine phosphorylation during capacitation. Vizel *et al.,* 2015 DOI: 10.1016/j.bbagen.2015.06.005	0.0886
Uncharacterized protein Accession: A0A287BR23	DUF4685 domain-containing protein. No characterized function. www.uniprot.org	0.0914
Angiotensin-converting enzyme GN: ACE	Zinc metallopeptidase, membrane protein. Important for sperm transport through the oviduct and sperm-zona pellucida binding. Likely involved in the distribution of ADAM3 for zona binding. Yamaguchi *et al.,* 2006 DOI: 10.1095/biolreprod.106.052977	0.094
Uncharacterized protein Accession: K7GM09	Integral component of membrane. Protein appears like: Calponin-homology domain-containing protein. www.uniprot.org	0.0956
Outer dense fiber protein 1 GN: ODF1	Sperm structural protein, crucial for proper head attachment and normal connecting piece morphology. Schneider *et al.,* 2016 DOI: 10.1074/mcp.M116.060343	0.0959
Family with sequence similarity 71 member D GN: FAM71D	Associated with sperm motility and is found in sperm flagella. Ma *et al.,* 2017 DOI: 10.1093/humrep/dex290	0.0962
Chromosome 3 open reading frame 84 GN: C3orf84	HDNR domain-containing protein. No described function. www.uniprot.org	0.0977
Uncharacterized protein GN: NDUFA7	Mitochondrial protein, part of Complex I in the electron transport chain. Alston *et al.,* 2018 DOI: 10.1016/j.ajhg.2018.08.013	0.0983
Uncharacterized protein GN: GK	Converts glycerol to glycerol-3-phosphate. www.uniprot.org	0.0985

Table 2: Proteomic identification of mitophagy and sperm remodeling cofactors in porcine cell-free system after 24 hours of co-incubation.

Protein of Interest Legend: GN = Gene name PE = protein existence level SV = Sequence version (PE and SV only included for proteins which had multiple versions in the table)	Proposed role in autophagy/mitophagy/post-fertilization sperm structure remodeling by zygote, and original references describing identified proteins' role in those events.	P value based off 3 rep T-test analysis
CLASS 1 – Proteins detectable on spermatozoa only after extract exposure.		
Zona pellucida sperm-binding protein 3 GN: ZP3	Involved in sperm-egg recognition, acrosomal reaction, and polyspermy defense. Zimmerman *et al.,* 2011 DOI: 10.1371/journal.pone.0017256	0.0001
Metalloendopeptidase a.k.a. Ovastacin GN: ASTL	Member of peptidase family involved in reproductive protein processing in *Drosophila;* (ov)astacin is secreted by mouse oocyte to cleave zona, prevent polyspermy. Ram *et al.,* 2006 DOI: 10.1073/pnas.0606228103 ; Burkart *et al.,* 2012; DOI: 10.1083/jcb.201112094	0.0002
Uncharacterized protein GN: PRDX3	Necessary for normal mitochondrial function. Localizes to the mitochondria after peroxide exposure and acts as a peroxide reducing agent. Wonsey *et al.,* 2002 DOI: 10.1073/pnas.102523299	0.001
Zona pellucida sperm-binding protein 4 GN: ZP4	Involved in sperm-egg recognition, acrosomal reaction, and polyspermy defense. Zimmerman *et al.,* 2011 DOI: 10.1371/journal.pone.0017256	0.1837

Small Calcium-binding mitochondrial carrier 1 GN: SCAMC	Protein involved in ATP-Mg/Pi transport across the inner mitochondrial membrane, in a calcium regulated manner. Arco & Satrustegui 2004 DOI: 10.1074/jbc.M401417200	0.1839
Lactamase beta GN: LACTB	Localized to the intermembrane space of the mitochondria. Forms long, stable filaments to create intramitochondrial membrane organization and micro-compartments within the mitochondria. Polianskyte *et al.,* 2009 DOI: 10.1073/pnas.0906734106	0.1844
Nucleophosmin/nucleoplasmin 2 GN: NPM2	Sperm nucleus remodeling after fertilization. Required for histone import into paternal pronucleus. McLay & Clark., 2003 DOI: 10.1530/rep.0.1250625	0.1861
Zona Pellucida sperm-binding protein 2 GN: ZP2	Involved in sperm-egg recognition, acrosomal reaction, and polyspermy defense. Zimmerman *et al.,* 2011 DOI: 10.1371/journal.pone.0017256	0.1875
Peptidyl arginine deiminase 6 GN: PADI6	Essential for early zygotal development, specifically cytoskeletal sheet formation through citrullination. Essential for female fertility. Esposito *et al.,* 2007 DOI: 10.1016/j.mce.2007.05.005	0.1875
Major Vault Protein GN: MVP	Regulates cell growth and survival through the STAT3 and Akt signaling pathways. Das *et al.,* 2016 DOI: 10.1016/j.cellsig.2015.10.007	0.1889
CLASS 2 - Detected in the vehicle and primed control spermatozoa, increased in extract-exposed spermatozoa.		
Uncharacterized protein GN: HMGB3	Positively regulates transcription through RNA polymerase II. Located in the nucleus. www.uniprot.org	0.0039
Myeloid leukemia factor 1 GN: MLF1	Negatively regulates the HOP mitochondrial protein complex to regulate cell survival. Serves as a proapoptotic antagonist. Sun *et al.,* 2017 DOI: 10.1016/j.bbamcr.2017.01.016	0.005
PHD finger protein 7 GN: PHF7	Plays a role in histone-to-protamine exchange during spermiogenesis. Appears to begin the ubiquitylation of H2A in round spermatids. Wang *et al.,* 2019 DOI: 10.1242/dev.175547	0.0063
Spermatogenesis associated 24 GN: SPATA24	DNA binding protein. Located in cytosol and nucleus. www.uniprot.org	0.0122
Uncharacterized protein GN: C12H17orf100	No characterized function www.uniprot.org	0.0315
Ubiquitin specific peptidase 50 GN: USP50	A deubiquitinating enzyme which regulates the cell cycle through prevention of Wee1 degradation. USP50 interacts with HSP90 and accumulates after DNA damage. It's believed to prevent entry into mitosis following DNA damage. Aressy *et al.,* 2010 DOI: 10.4161/cc.9.18.13133	0.0333
Proteasome subunit alpha type GN: PSMA8	A testis specific proteasomal subunit found during spermatogenesis. Appears crucial for proper meiotic exit by the forming spermatids. Gomez-H *et al.,* 2019 DOI: 10.1371/journal.pgen.1008316	0.046
Chromosome 2 open reading frame 70 GN: C2orf70	No characterized function www.uniprot.org	0.0487
Theg spermatid protein GN: THEG	Testicular haploid expressed gene. Thought to only be expressed in spermatid cells. Though not essential for spermatogenesis it is thought to participate in	0.0872

	Sertoli cell and spermatid interactions. Mannan *et al.,* 2003 DOI: 10.1095/biolreprod.103.017400	
Proteasome assembly chaperone 2 GN: PSMG2	Interacts closely with PAC1 and they help ensure proper proteasome core formation, acting as a quality control mechanism. Wu *et al.,* 2018 DOI: 10.1111/gtc.12631	0.0878
CLASS 3 – Proteins detected in spermatozoa before extract, reduced after extract exposure.		
Creatine Kinase B-type GN: CKB	Part of the phosphocreatine biosynthetic pathway. Binds ATP and produces N-phosphocreatine. www.uniprot.org	0.000043
Platelet-activating factor acetylhydrolase IB subunit alpha GN: PAFAH1B1	Plays a role in spermatogenesis and is found in the acrosome and midpiece of spermatozoa. However, it is also found in the membrane of oocytes and zygotes. Yao *et al,* 2015 DOI: 10.1016/j.rbmo.2015.07.010	0.0039
Electron transfer flavoprotein subunit beta GN: ETFB	Mitochondrial protein that is part of the electron transport chain. Serves as an electron acceptor molecule. Schmiesing *et al,* 2014 DOI: 10.1371/journal.pone.0087715	0.0121
Chromosome 17 open reading frame 98 GN: C17orf98	No characterized function. www.uniprot.org	0.0121
Glutamate-cysteine ligase modifier subunit GN: GCLM	Regulates mitochondrial depolarization and participates in the glutathione biosynthetic pathway. www.uniprot.org	0.0125
Serotransferrin GN: TF	Modulates interactions between endosomes and mitochondria. Das *et al.,* 2016 DOI: 10.1083/jcb.201602069	0.0177
L-lactate dehydrogenase B chain GN: LDHB	When deacetylated by SIRT5, autophagy is promoted. Shi *et al.,* 2019 DOI: 10.1002/1878-0261.12408	0.0184
Uncharacterized protein GN: LOC396905	Sperm-associated acrosin inhibitor isoform X1. No characterized function. www.uniprot.org	0.0199
Receptor of activated protein C kinase 1 GN: RACK1	Ribosomal protein located on the small ribosomal subunit and appears to regulate translation. Gallo *et al.,* 2018 DOI: 10.1128/MCB.00230-18	0.0203
Radial spoke head 14 homolog GN: RSPH14	No characterized function. www.uniprot.org	0.0218
Eukaryotic translation initiation factor 4E GN: EIF4E	Reduces an apoptotic susceptibility via an inhibition of mitochondrial cytochrome c release. Li *et al.,* 2003 DOI: 10.1074/jbc.M208821200	0.024
Lactotransferrin GN: LTF	Iron-binding glycoprotein. Regulates iron absorption, & immune responses. Hao *et al.,* 2019 DOI: 10.2174/1389203719666180514150921	0.0279
Transducin beta like 2 GN: TBL2	Localizes to the endoplasmic reticulum and interacts with the 60S ribosomal subunit. Also works with PERK during ER stress. Tsukumo *et al,* 2015 DOI: 10.1016/j.bbrc.2015.04.144	0.0312
Histone H2A GN: HIST2H2AB	A histone 2A variant which confers specific properties to the nucleosome. Plays a dominant role in chromatin dynamics and function. Osakabe *et al.,* 2018 DOI: 10.1093/nar/gky540	0.0342
Adenylate cyclase 3 GN: ADCY3	Required for normal spermatozoa function. Plays a role in male fertility and appears to localize to the acrosomal membrane, may play a role in the acrosomal reaction. Livera *et al.,* 2005 DOI: 10.1210/me.2004-0318	0.0358
Retinoic acid receptor responder 1 GN: RARRES1	Metalloendopeptidase inhibitor activity, found in the extracellular matrix. www.uniprot.org	0.0401
Spermatogenesis-associated protein 20 GN: SPATA20	Participates in DNA damage response in male germ cells. Facilitates DNA repair. Zheng *et al.,* 2017 DOI: 10.1371/journal.pone.0178535	0.0469

ADP ribosylation factor like GTPase 1 GN: ARL1	Involved in endosomal trans-Golgi network and secretory traffic, lipid droplet formation, innate immunity, stress tolerance and unfolded protein response. Yu & Lee 2017 DOI: 10.1242/jcs.201319	0.0536
Glycerol-3-phosphate dehydrogenase (NAD[+]) GN: GPD1L	Converts glycerol 3-phosphate into dihydroxyacetone phosphate. Part of the carbohydrate metabolic process. www.uniprot.org	0.0563
G protein subunit beta 2 GN: GNB2	Binds the G-protein gamma-subunit & GTPases. Part of the G protein-coupled receptor signaling pathway. www.uniprot.org	0.0593
IQ motif containing F2 GN: IQCF2	Binds calmodulin. www.uniprot.org	0.0623
RAB3B member RAS oncogene family GN: RAB3B	Involved in various cellular pathways. Has GTPase activity and binds myosin. www.uniprot.org	0.0634
Uncharacterized protein GN: MS4A14	Found during spermatogenesis in round spermatids to spermatozoa. Localized to the acrosome and midpiece. Involved in fertilization and zygotic division. Xu *et al.,* 2014 DOI: 10.1530/REP-14-0087	0.0643
Keratin 14 GN: KRT14	Part of the intermediate filament portion of the cytoskeleton. www.uniprot.org	0.0673
Endosome associated trafficking regulator 1 GN: ENTR1	Controls Fas-mediated apoptotic signaling via binding to Dysbindin. Sharma *et al.,* 2019 DOI: 10.1038/s41467-019-11025-y	0.0691
NME/NM23 family member 5 GN: NME5	Involved in spermatid development, flagellum assembly, and acts as a nucleoside diphosphate kinase. www.uniprot.org	0.07
Deoxythymidylate kinase GN: DTYMK	Part of the mitochondrial nucleotide salvage pathway. Mutations in this gene cause mitochondrial DNA depletion syndrome. Lam *et al.,* 2019 DOI: 10.1016/j.cca.2019.06.028	0.0714
Rho GDP dissociation inhibitor alpha GN: ARHGDIA	Regulates protein localization, part of the Rho and semaphoring-plexin signaling pathways. www.uniprot.org	0.0722
Thioredoxin domain containing 17 GN: TXNDC17	Peroxidase and protein-disulfide reductase activities. www.uniprot.org	0.0756
Keratin 7 GN: KRT7	Part of the keratin-based cytoskeleton. www.uniprot.org	0.0777
Uncharacterized protein Accession: A0A287BM70	UPAR/Ly6 domain-containing protein. www.uniprot.org	0.0796
Uncharacterized protein GN: LOC100738961	No characterized function. www.uniprot.org	0.0827
GTP-binding protein SAR1a GN: SAR1A	Part of the COPII-coated vesicle transporting system. GTPase activity. www.uniprot.org	0.0834
ATP binding cassette subfamily E member 1 GN: ABCE1	Undergoes ubiquitination by NOT4 in response to mitochondrial damage. Acts as translational quality control. Showing that PINK1-directed mitophagy influences translation in cells. We *et al.,* 2018 DOI: 10.1016/j.cmet.2018.05.007	0.0856
Sarcoplasmic/endoplasmic reticulum calcium ATPase 2 GN: ATP2A2	Plays roles in calcium ion homeostasis, organelle organization, response to oxidative stress and ER transport. www.uniprot.org	0.0876
Uncharacterized protein GN: LOC100515166	IF rod domain-containing protein. A structural protein, part of the intermediate filaments. www.uniprot.org	0.0891
60S acidic ribosomal protein P0 GN: RPLP0	When depleted, PLAAT4 induced cell cycle arrest and cell death are increased. Wang *et al.,* 2019 DOI: 10.1007/s12013-019-00876-3	0.0891

Tctex-type 1 dynein light chain GN: DYNLT1	Necessary for male germ cell development. Known to be involved in protein trafficking, membrane vesiculation, cell cycle regulation and stem cell differentiation. Indu *et al.,* 2015 DOI: 10.1074/mcp.M115.050005	0.0959
Uncharacterized protein Accession: F1SL35	Glutathione transferase. Part of the glutathione metabolic process. www.uniprot.org	0.0977
Eukaryotic translation elongation factor 2 GN: EEF2	Catalyzes reverse localization of the ribosome. Susorov *et al.,* 2018 DOI: 10.1074/jbc.RA117.000761	0.0982
Uncharacterized protein GN: ZG16B	Depletion increases aneuploidy, promotes apoptosis, and activates the Wnt/Beta-catenin pathway. Escudero-Paniagua *et al.,* 2020 DOI: 10.1093/carcin/bgz093	0.0991
Uncharacterized protein GN: KRT8	When phosphorylated, this protein induces autophagy impairment by affecting the fusion of autophagosomes and lysosomes. Miao *et al.,* 2020 DOI: 10.1111/jcmm.14998	0.0994
NADH:ubiquinone oxidoreductase core subunit S8 GN: NDUFS8	Part of complex I in the mitochondrial respiratory chain. www.uniprot.org	0.0997

Investigation of candidate proteins in the porcine cell-free system

Six candidate proteins were selected from the mass spectrometry results for further investigation. These six proteins were MVP, PSMG2, PSMA3, FUNDC2, SAMM50, and BAG5. Western blot detection and immunocytochemistry were used to describe the presence and localization patterns of these candidate proteins in ejaculated, primed, and cell-free treated spermatozoa. Furthermore, immunocytochemistry was used to observe the localization of these proteins in *in vitro* derived porcine zygotes. Oocytes were fertilized with spermatozoa pre-labeled with MitoTracker so that mitochondrial sheaths could be detected. These oocytes, now presumed zygotes, were then collected at 15 and 25 hours post insemination (sperm and oocytemixing). These time points were selected to ensure that post-fertilization sperm mitophagy was well underway in the zygotes at both timepoints. Furthermore, the 25 hour time point was selected to observe the advanced stages of mitophagy post-gamete mixing. These presumed zygotes were then fixed and stained for immunocytochemistry.

MVP

Major vault protein was identified as a Class 1 protein of interest in our MS trials. It was not identified in vehicle control spermatozoa or primed control sperm samples. However, it was identified in oocyte extracts and in spermatozoa exposed to the cell-free system at both the 4- and 24-hour times points. Upon further investigation we confirmed that MVP was not detected in ejaculated spermatozoa by using both Western blotting and immunocytochemistry detection methods (**Figure 3A, B**). Additionally, after priming the spermatozoa, MVP was still not detected (**Figure 3C**). However, consistent with MS observations, MVP was detected on the tails of treated spermatozoa after both 4 and 24 hours of cell-free system exposure (**Figure 3D, E**). In zygotes 15 hours post insemination MVP was detected abundantly in the cytoplasm as reported previously (Sutovsky et al., 2005) though it did not appear to be associating with forming male pronuclei (PN) or with the mitochondrial sheaths of the fertilizing spermatozoa (**Figure 3F**). At 25 hours post insemination, MVP was still detectable in the cytoplasm of the zygote and did appear to have colocalization on the MS of the fertilizing spermatozoa (**Figure 3G**).

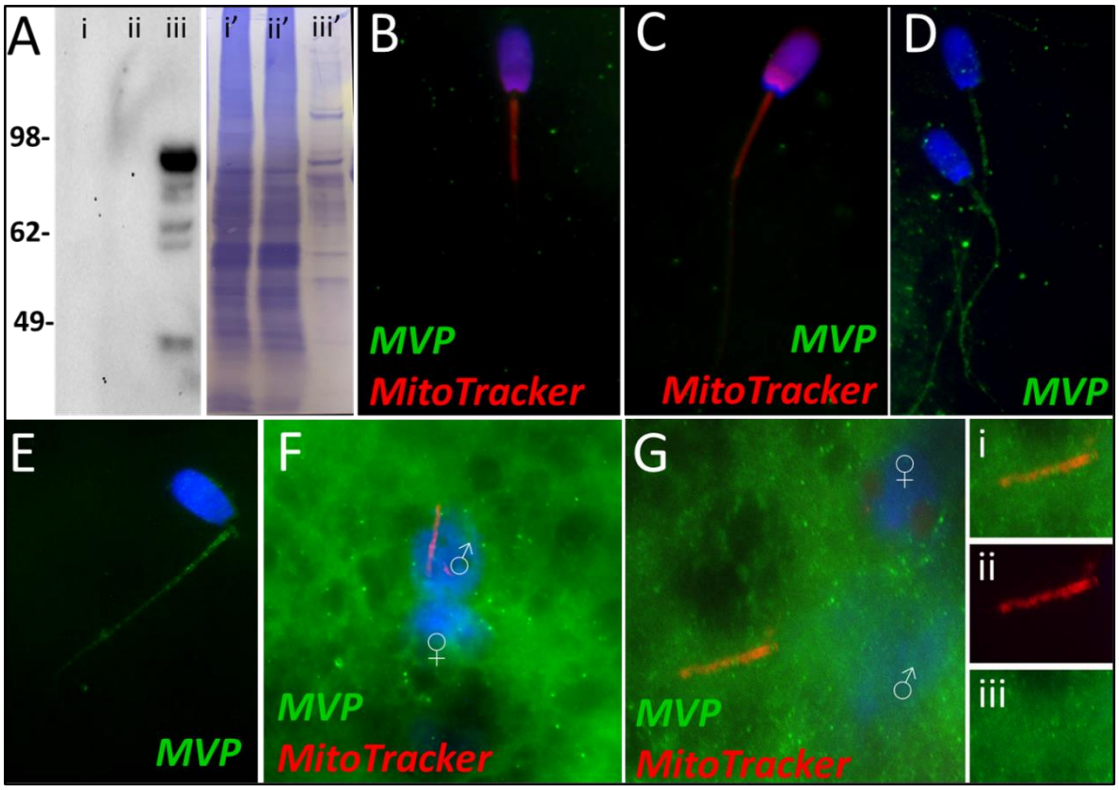

Figure 3. MVP in the porcine cell-free system. Major vault protein was not detected in ejaculated (Lane i) or capacitated spermatozoa (Lane ii) via Western blot detection, but it was detected in oocytes (Lane iii) (**A**; predicted mass = 99 kDa); (Lanes i', ii', iii') On the right side of panel A, PVDF membrane stained with Coomassie brilliant blue after chemiluminescence detection shows protein loads within each lane. MVP was not detected in ejaculated (**B**) or primed spermatozoa (**C**) via immunocytochemistry. After both 4 and 24 hours of cell-free system exposure, MVP (green) was then detected throughout the tail of the treated spermatozoa (**D** and **E**). MVP was detected in the cytoplasm of zygotes 15 hours post insemination but did not appear to associate with the pronuclei or MS (**F**). MVP was still detected in the cytoplasm of zygotes 25 hours post insemination and did appear to have some association with the MS of the fertilizing spermatozoa (**G**). A zoomed in cutout of the MS can be found in (**Gi**). The MS is shown by MitoTracker labeling in red channel separation panel (**Gii**). The green/protein labeling channel separation is shown in (**Giii**).

PSMG2

During our MS trials, proteasome assembly chaperone 2 was identified as a Class 2 protein during the 24-hour trial. PSMG2 was found to undergo a significant increase in abundance after 24 hours in the cell-free system ($p=0.088$). However, during the 4-hour trial, PSMG2 increased during two of the replicates but underwent a decrease in one of the replicates and was thus not found to be significant. PSMG2 was detected in ejaculated spermatozoa via WB (**Figure 4A**) and found to localize to the acrosome of ejaculated spermatozoa (**Figure 4B**). After priming, PSMG2 was still detected in the head of spermatozoa (**Figure 4C**). After 4 hours of cell-free system co-incubation PSMG2 was detected in both the head and principal piece of the sperm tail. (**Figure 4D**). After 24 hours of cell-free system exposure, this tail localization was no longer present and PSMG2 is found only on the partially decondensed (as a result of oocyte extract inducing sperm nucleus remodeling) heads of the spermatozoa (**Figure 4E**). When observed in zygotes 15 hours post insemination PSMG2 had begun to cluster around the newly forming paternal, sperm-derived pronuclei (**Figure 4F**). At 25 hours post insemination, a robust cluster of PSMG2 was detected surrounding the male pronuclei and on the mitochondrial sheath of the fertilizing spermatozoa (**Figure 4G**).

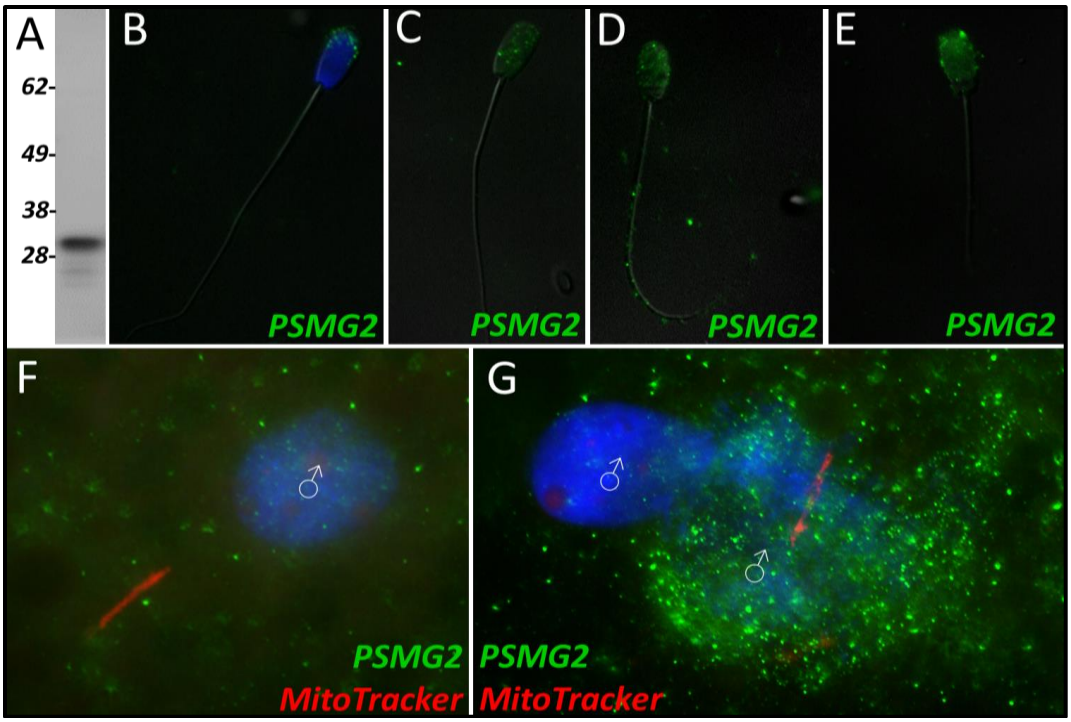

Figure 4. PSMG2 in the porcine cell-free system. Proteasomal assembly chaperone 2 was detected in ejaculated spermatozoa using Western blotting (**A**; predicted mass = 29 kDa), and immunocytochemistry (green) (**B**), where it was found to localize to the acrosome. In primed spermatozoa, PSMG2 was spread throughout the entire head (**C**). After 4 hours of cell-free system exposure, this same localization pattern was detected in the sperm head, but PSMG2 was also localized to the principal piece of the tail (**D**). After 24 hours of cell-free system exposure, PSMG2 was only detected in the head of the treated spermatozoa (**E**). PSMG2 was detected around the new forming paternal pronuclei in zygotes 15 hours post insemination (**F**). PSMG2 is detected robustly localizing to the paternal pronuclei and the MS of the fertilizing spermatozoa in this polyspermic zygote, 25 hours post insemination (**G**). Note that the larger, more developed PN on the right has the majority of the PSMG2 labeling.

PSMA3

Proteasome subunit alpha 3 significantly increased (p=0.015) during the 4-hour MS trials and was categorized as a Class 2 protein. During our 24-hour MS trial, PSMA3 was found to undergo an increase during two of the replicates but displayed a decrease in one of the replicates. PSMA3 was detected in ejaculated spermatozoa by using both WB (**Figure 5A**) and immunocytochemistry detection (**Figure 5B**); it was found to localize to the acrosome of the ejaculated spermatozoa. After priming, PSMA3 was found in the tail of the spermatozoa, including midpiece and principal piece (**Figure 5C**). This localization pattern persisted after 4 hours of cell-free system exposure (**Figure 5D**). After 24 hours of cell-free system exposure, PSMA3 was still detected throughout the tail but with a more focused/prevalent localization pattern on the MS (**Figure 5E**). In zygotes 15 hours post insemination PSMA3 clustered around the nascent paternal pronuclei and on the mitochondrial sheath of the fertilizing spermatozoa (**Figure 5F**). This same localization pattern persisted 25 hours post insemination and PSMA3 continued to cluster near the male and female pronuclei and on the MS of fertilizing spermatozoa (**Figure 5G**).

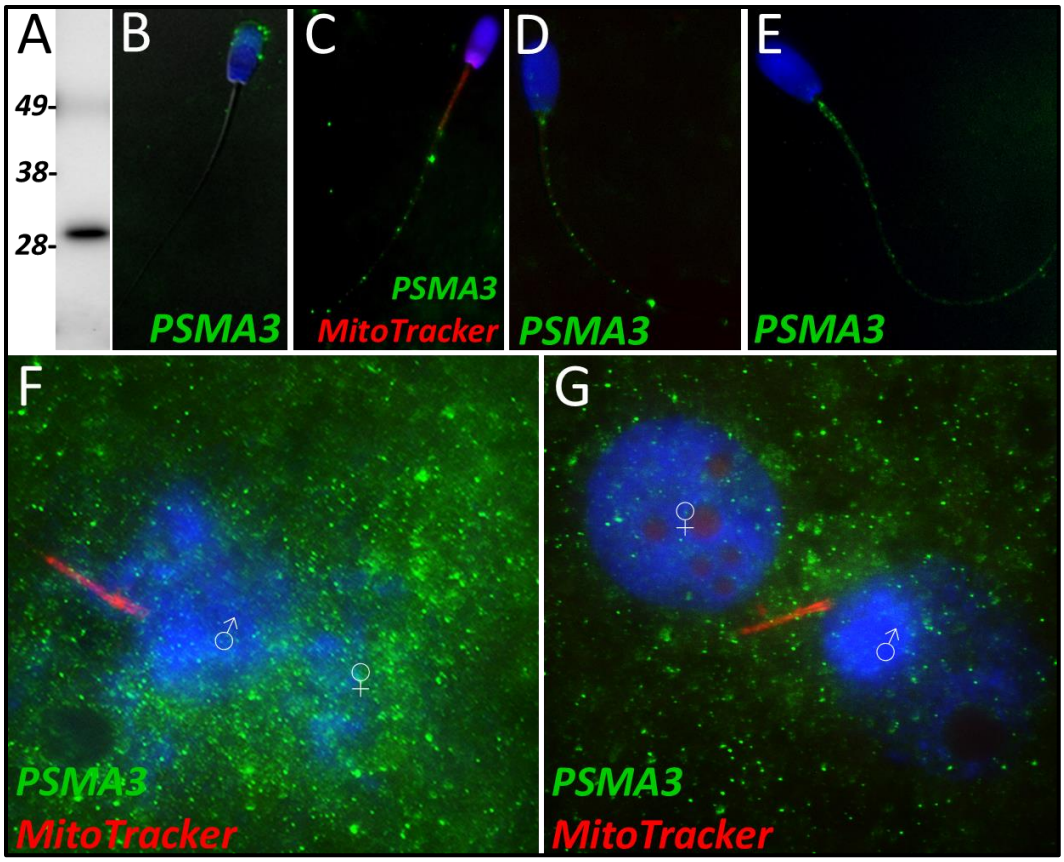

Figure 5. PSMA3 in the porcine cell-free system. Proteasomal subunit alpha 3 was detected in ejaculated spermatozoa via Western blotting detection (**A**; predicted mass = 28.4 kDa). PSMA3 (green) was localized to the acrosome of ejaculated spermatozoa by immunocytochemistry (**B**). After the priming process, PSMA3 was detected in the tail of primed spermatozoa (**C**). This same tail localization pattern was observed after both 4 and 24 hours of cell-free system exposure (**D** and **E**). PSMA3 was detected in zygotes both 15 and 25 hours post insemination (**F** and **G**); it was detected surrounding the male and female pronuclei as well as on the mitochondrial sheath of the fertilizing spermatozoa.

FUNDC2

FUN14 domain-containing protein 2, a Class 3 protein in our classification, was observed to undergo a significant decrease in abundance after 4 hours of cell-free system exposure (p=0.084). No significant change in the abundance of FUNDC2 was detected during the 24-hour trial. During our 24-hour MS trial, FUNDC2 was found to undergo a reduction during two of the replicates but displayed a slight increase in one of the replicates. FUNDC2 was detected in ejaculated spermatozoa via WB detection (**Figure 6A**). In ejaculated spermatozoa, FUNDC2 was detected in the acrosome and equatorial segment of the sperm head and was confined to MS within the sperm tail (**Figure 6B**). After sperm capacitation, FUNDC2 changed its localization and was found primarily in the apical ridge of the acrosome but also in the MS (**Figure 6C**). After the removal of disulfide bonds via priming, FUNDC2 was predominantly detected in the MS of primed spermatozoa compared to ejaculated and capacitated spermatozoa and was still detected on the remnants of the acrosome (**Figure 6D**). Upon 4 hours of cell-free system exposure, FUNDC2 was found to localize throughout the entire tail of the spermatozoa (**Figure 6E**). Interestingly, after 24 hours of cell free system exposure, FUNDC2 was again confined to the MS of the spermatozoa but appeared to have a fractured pattern, perhaps revealing the remaining mostly intact mitochondria or vice versa, i.e., it may be localized to those mitochondria which have undergone the greatest degree degradation at this time point (**Figure 6F**).

FUNDC2 was not detected on or near the fertilizing spermatozoa at 15 hours post insemination (**Figure 6G**); in contrast FUNDC2 was still detected in the head and tail of a spermatozoa bound to the zona pellucida of a zygote at the same time point (**Figure 6H**). FUNDC2 was also not observed localizing on or near the fertilizing spermatozoa at 25 hours post insemination but was detected in non-fertilizing, zona bound spermatozoa at the same time point (**Figure 6I,J**).

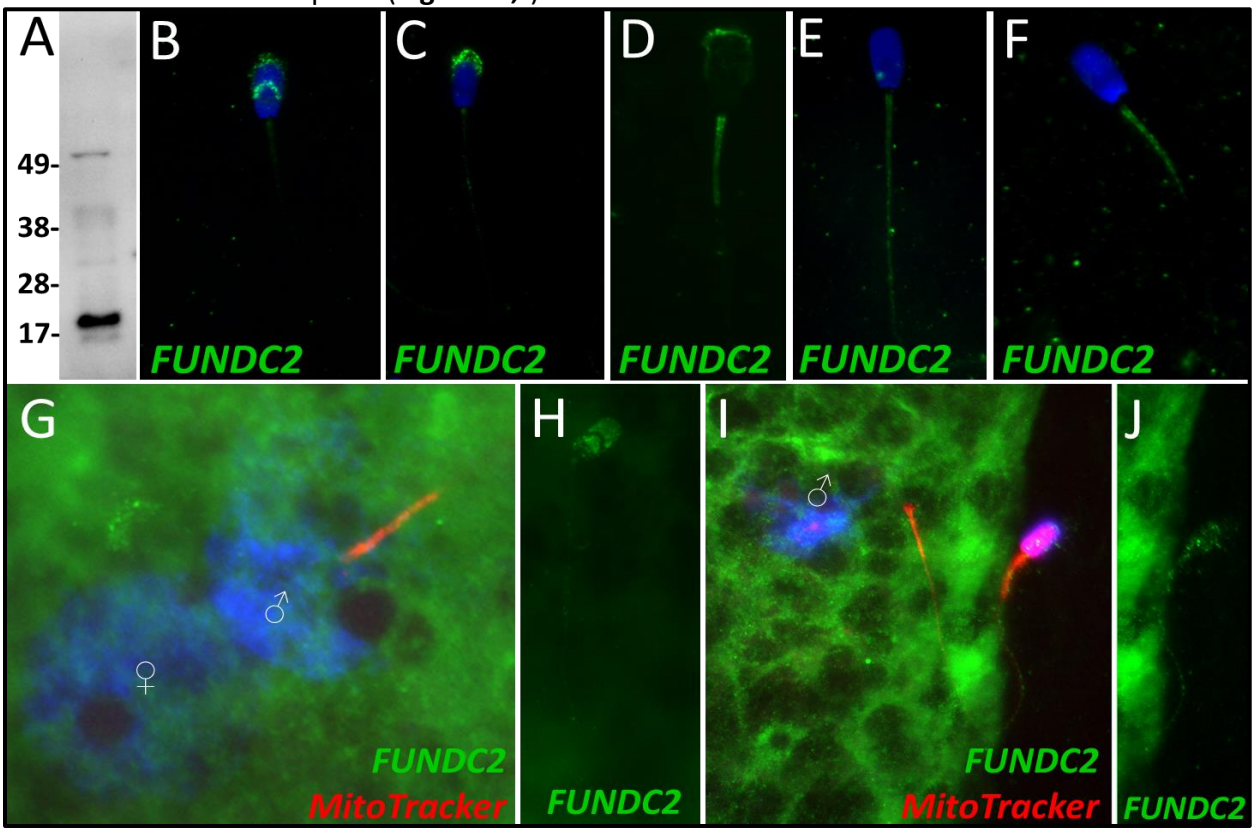

Figure 6. FUNDC2 in the porcine cell-free system. FUN14 domain-containing protein 2 was detected in ejaculated spermatozoa by Western blotting (**A**; predicted mass = 20.7 kDa). FUNDC2 was detected in the acrosome and equatorial segment of ejaculated spermatozoa (**B**) and the acrosome and MS of capacitated spermatozoa (**C**). In primed spermatozoa, FUNDC2 was detected in the MS and the remnants of the acrosome (**D**). After 4 hours of cell-free system exposure, FUNDC2 was detected throughout the tail of the treated spermatozoa (**E**), and after 24 hours of cell-free system exposure, FUNDC2 was detected in the MS of treated spermatozoa (**F**). FUNDC2 was not detected localizing to the fertilizing sperm components in zygotes 15 hours post insemination (**G**). In contrast, a zona bound spermatozoa at that same time point had FUNDC2 localized throughout the head and some tail localization as well (**H**). FUNDC2 was not detected localizing to the fertilizing sperm components in zygotes 25 hours post insemination (**I**), but a non-fertilizing spermatozoon bound to the oolemma at this same time point still had some FUNDC2 labeling in its tail and head, as shown by a fluorescent channel separated cutout (**J**).

SAMM50

Sorting and assembly machinery component 50 was observed to undergo a significant decrease in abundance during the 4-hour MS trial (p=0.035), classifying it as a Class 3 protein. This decrease in abundance was not observed during the 24-hour MS trial wherein SAMM50 underwent a reduction within two of the replicates but underwent a slight increase in one of the replicates. SAMM50 was detected in spermatozoa via WB and immunocytochemistry (**Figure 7A and B**); it was found to localize to the acrosome and MS of the sperm tail. After priming, this same localization pattern persisted on the MS and in what remained of the acrosome and appeared to localize to the principal piece as well (**Figure 7C**). After 4 hours of co-incubation within the cell-free system, SAMM50 was completely removed from the remnants of the acrosome, but still

found throughout the tail with the greatest density of localization on the MS as seen in primed spermatozoa as well, due to acrosome removal by priming (**Figure 7D**). This same localization pattern was observed after 24 hours of cell-free system co-incubation (**Figure 7E**). During our zygote trial, SAMM50 was observed localizing on and near the MS of the fertilizing spermatozoa at 15 hours post insemination (**Figure 7F**). SAMM50 was also detected 25 hours post insemination localizing to the principal piece of the fertilizing spermatozoa, but no longer on the MS (**Figure 7G**).

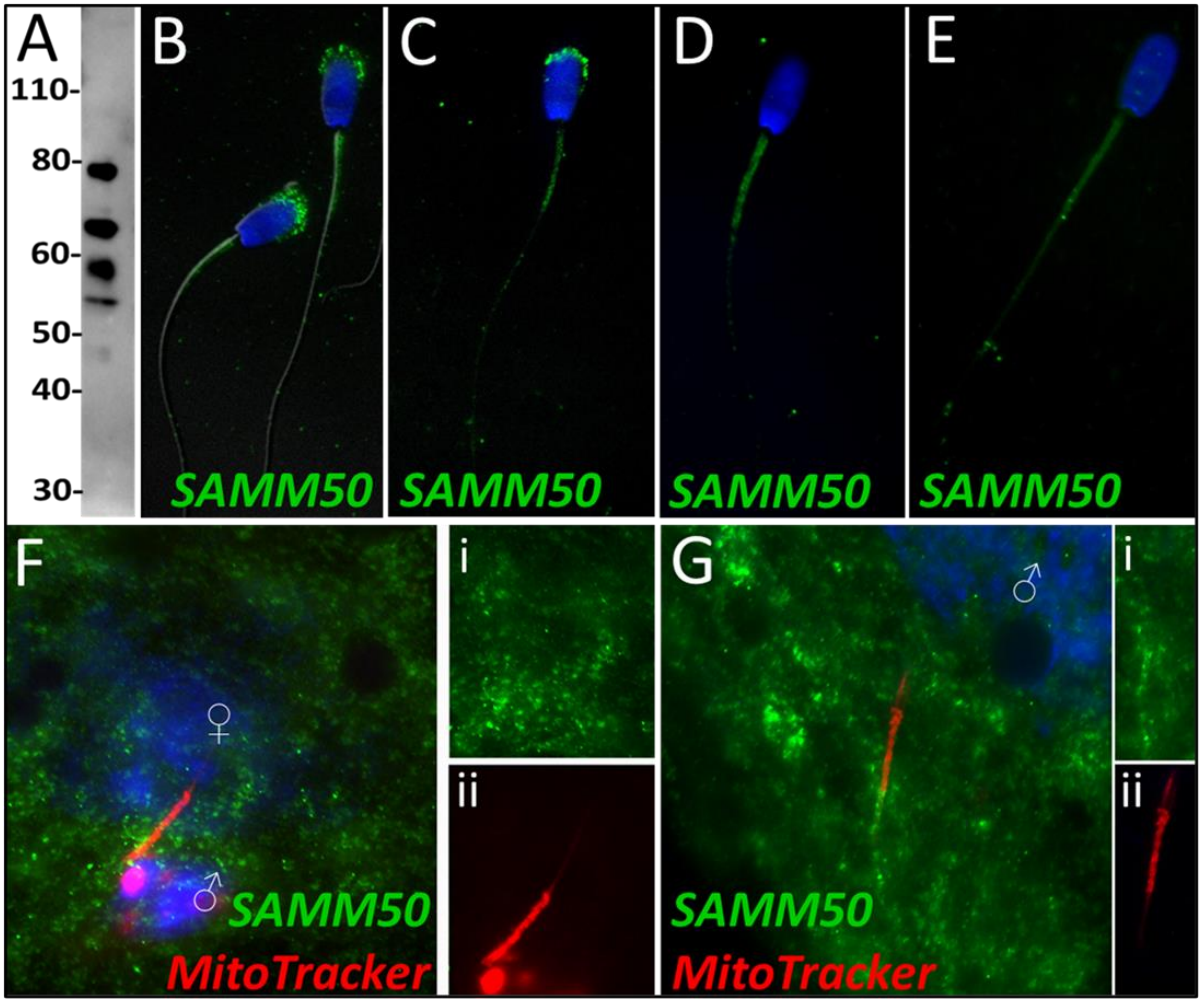

Figure 7. SAMM50 in the porcine cell-free system. Sorting and assembly machinery component 50 was detected in ejaculated spermatozoa using Western blotting (**A**; predicted mass = 51 kDa). SAMM50 has predicted post translational modifications, including phosphorylation sites and ubiquitination sites, as predicted using the MuSite Deep prediction software which likely explains the higher bands which are observed. SAMM50 was also detected in ejaculated spermatozoa using immunocytochemistry and found to localize to the acrosome and the MS of the sperm tail (**B**). In primed spermatozoa, SAMM50 was detected in the remnants of the acrosome, as well as in the MS, and the principal piece (**C**). After 4 hours of cell-free system exposure, SAMM50 was detected predominantly in the MS with some signal present in the principal piece of the sperm tail as well (**D**). After 24 hours of cell-free system exposure, SAMM50 was detected in predominantly in the MS, still with residual principal piece labelling as well (**E**). SAMM50 was detected in zygotes 15 hours post insemination (**F**). It was detected on and near the MS of the fertilizing spermatozoa. Fluorescence channel separation cutouts of the MS and principal piece is shown in (**Fi**; green SAMM50) and (**Fii**; red MitoTracker). SAMM50 was also detected in zygotes 25 hours post insemination (**G**). It was detected on the principal piece of the tail of the fertilizing spermatozoa, just below the MS. Fluorescence channel separation cutouts of the MS and principal piece remnants is shown in (**Gi**; green SAMM50) and (**Gii**; red MitoTracker).

BAG5

Based on quantitative proteomics, BAG family molecular chaperone regulator 5 underwent a decrease in abundance during the 4-hour MS trial (p=0.02). However, this level of significance was not observed during the 24-hour MS trial. During our 24-hour MS trial, BAG5 underwent a reduction during two of the replicates but a slight increase in one of the replicates. Upon further investigation, BAG5 was detected by Western blotting (**Figure 8A**) and immunocytochemistry (**Figure 8B**) in fresh ejaculated spermatozoa, where it was localized exclusively to the acrosome. After priming, BAG5 was only detectable in the remains of the acrosome and weakly on the sperm tail (**Figure 8C**). After 4 hours of co-incubation within the cell-free system, BAG5 was no longer detected on the head of the spermatozoa but became detectable on the MS of the spermatozoa (**Figure 8D**). Likewise, after 24 hours of co-incubation within the cell-free system, this same BAG5 localization to the MS remained(**Figure 8E**). BAG5 was not observed localizing on the fertilizing spermatozoa 15 hours post insemination, though BAG5 did appear to be present in the cytoplasm of the zygote (**Figure 8F**). In zygotes at 25 hours post insemination, BAG5 was still not observed on the fertilizing spermatozoa, but remained present within the cytoplasm of the zygote (**Figure 8G**).

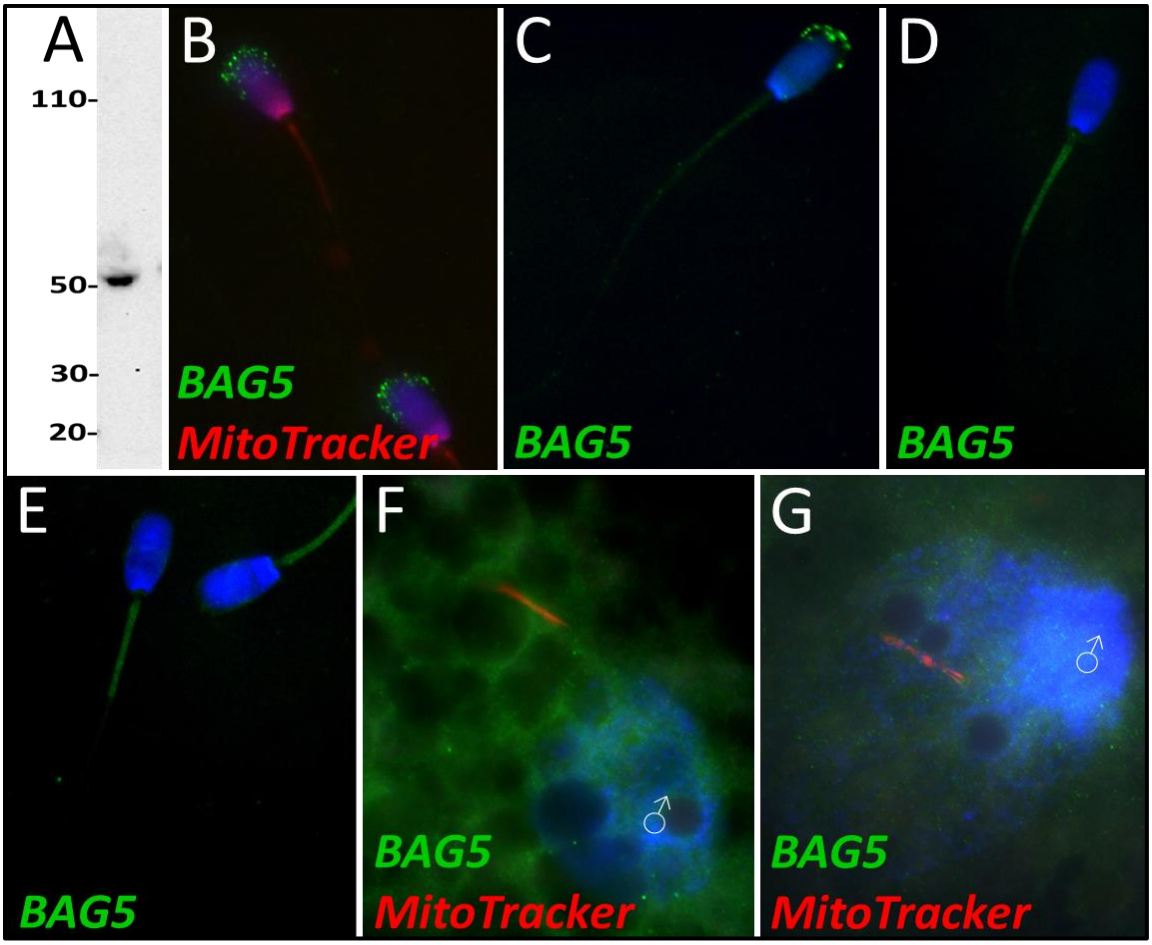

Figure 8. BAG family molecular chaperone regulator 5 was detected in ejaculated spermatozoa via WB (**A**; predicted mass = 54 kDa) and immunocytochemistry (**B**), where it was detected to localize in the acrosome. After priming, BAG5 still remained localized to what remained of the acrosome (**C**). After 4 and 24 hours of cell-free system exposure, BAG5 was detected in the MS of the treated spermatozoa (**D** and **E**). BAG5 was detected in the cytoplasm in zygotes 15 hours post structures (**F**) and 25 hours post fertilization, with no obvious association with the fertilizing sperm structures or their remnants (**G**).

Discussion

In the last decade, considerable effort has been put forth to better understand the autophagic pathway's involvement in mitochondrial inheritance (Al Rawi et al., 2011; Politi et al., 2014; Sato & Sato, 2011; W. H. Song et al., 2016; Zhou et al., 2011). Much headway has been made; however, the knowledge gaps surrounding this post-fertilization sperm mitophagy process remain wide. For example, at present, it is not understood what determines species specificity or timing of sperm mitophagy. It has been observed that mammalian interspecies crosses retain the paternal mitochondria in F1 generation and become heteroplasmic as a result (Kaneda et al., 1995; Shitara, Hayashi, Takahama, Kaneda, & Yonekawa, 1998; P. Sutovsky et al., 1999). The timing of mitochondrial degradation in embryos also varies between species (Reviewed in (Zuidema & Sutovsky, 2019)). Additionally, many protein cofactors, substrates, and autophagic pathways which act within the post-fertilization mitophagic process remain to be identified. This area of research has relied on studies with mammalian oocytes and zygotes. This led to the development of our species-specific mammalian cell-free system (W. H. Song & Sutovsky, 2018). This system was developed to provide a new tool for the study of post-fertilization sperm mitophagy and other early fertilization events. Specifically, the use of this system in conjunction with quantitative mass spectrometry was a type of study which has never been attempted before, even though it is becoming increasingly popular to investigate sperm proteomes by using quantitative proteomic analyses(Baker et al., 2007; Martínez-Heredia, Estanyol, Ballescà, & Oliva, 2006; Pilatz et al., 2014; Zhang et al., 2022). Attempting to identify ooplasmic proteins which bind to spermatozoa at fertilization and those sperm proteins which begin degrading during fertilization by using mass spectrometry would be exceedingly difficult by using zygotes. This is because post-fertilization sperm mitophagy takes place within the oocyte cytoplasm and the ability to identify the differences in those proteins which are found in the sperm or binding the sperm surface from the rest of the oocyte proteome would be extremely challenging/impossible since we are not yet able to reliably map and quantify single cell proteomes. However, our cell-free system presents a unique tool which can be used to capture number of the early proteomic changes which take place specifically on the fertilizing spermatozoa; this cell-free system has been previously shown to mimic some early fertilization events (W.-H. Song et al., 2021; W. H. Song & Sutovsky, 2018). Thus, we could expect other proteomic events of early fertilization to be mimicked within our cell-free system. By using high-resolution mass spectrometry, we captured differences in relative protein abundance between primed control spermatozoa and cell-free treated spermatozoa. Furthermore, we captured this data at two different time points, i.e. after 4 hours and 24 hours of co-incubation within the cell-free system. Furthermore, we identified proteins of interest which can be further explored by using more targeted sperm phenotype studies.

This study was constrained to two time points, which allows for some temporal differences to be captured, but the differences over time in this cell-free system could be immense and the differences in the protein inventories compiled for each time point may be indicative of this. Furthermore, this cell-free system while useful does not perfectly capture all the events which take place during *in vivo* fertilization. The cell-free system is intended to mimic early fertilization events but is presumably not the exact same as *in vitro* fertilization. Furthermore, this study only captures changes in protein abundance. Proteins which remain at relatively stable abundances but undergo changes in localization and/or modification resulting in altered biological activity would not be captured by the parameters set forth in this study, but expectedly play important roles in early fertilization mechanisms. Despite these recognized limitations, this cell-free system used in conjunction with mass spectrometry allowed a glimpse into early fertilization proteomics in a way that has not been attempted before.

Our study ultimately identified 185 proteins which underwent a significant change in abundance within our parameters as described above (**Table S1**). Of these proteins, 144 were identified during the 4-hour cell-free system trial (**Table 1**) and 63 were found during the 24-hour cell-free system trial (**Table 2**), with 22 proteins overlapping between the trials. This lack of overlap was surprising but again may be reflective of our inability to truly detect the dynamic changes which take place within the cell-free system.

Considering the dynamic proteomic remodeling of both the oocyte and spermatozoa which takes place during early fertilization, these 185 proteins which have been identified likely play roles in processes beyond sperm mitophagy. Pathways related to pronuclear development, sperm aster formation, and degradation of the perinuclear theca, acrosome remnants, and tail structures including the mitochondrial sheath may all be captured. However, several autophagy-related proteins were found within our inventory including L-lactate dehydrogenase B chain, keratin 8, glycogen synthase kinase 3 beta 5, BAG family molecular chaperone regulator 5, sorting and assembly machinery component 50, and FUN14 domain-containing protein 2. Interestingly these proteins were all found in class 3, and thus these proteins may be mitophagy determinants or regulators which must be recognized by ooplasmic mitophagy receptors and removed from spermatozoa/sperm mitochondria for mitophagy to take place. In addition to these proteins, multiple components and regulators of the ubiquitin-proteasome system were also identified including 20S proteasomal subunits alpha type 2, 3, and 8, 26S proteasome non-ATPase regulatory subunit 2, 26S proteasome subunit ATPase 2, proteasome assembly chaperone 2, ubiquitin specific peptidase 50, E3 ubiquitin ligase cullin 4B and OTU deubiquitinase. These proteins are found in both classes 2 and 3; they may be involved in UPS-mediated mitophagy or play roles in the degradation of other sperm structures including the tail and perinuclear theca. There is also evidence of sperm proteasomes playing a role in acrosomal exocytosis, zona pellucida degradation, and events linked with sperm capacitation (Sutovsky, 2011; Zigo, Manaskova-Postlerova, Jonakova, Kerns, & Sutovsky, 2019; Zimmerman et al., 2011).

Class 1 proteins were proteins that were not identified within our primed control sperm proteome but were found in our cell-free system treated spermatozoa. We interpreted these as oocyte proteins which interacted with the oocyte extract exposed spermatozoa and remained bound to them after thorough washing at the end of co-incubation interval. Indeed, among the identified Class 1 proteins were several well documented oocyte-specific proteins which are known to interact with spermatozoa during early fertilization events, before or after sperm incorporation in the oocyte cytoplasm and are only found in oocytes. Adding to our confidence in the specificity of this cell-free proteomic system, these proteins included zona pellucida proteins 2, 3, and 4; ovastacin, DNA methyltransferase 1, and nucleoplasmin 2. Also, within Class 1, we observed proteins related to polyspermy prevention, pronuclear formation, cell development, and as well as several ROS scavenging proteins (**Figure 2A and B**). These pathways all reinforce known oocyte functions taking place during early fertilization events. Being able to capture some of these proteomic interactions is encouraging and shows that our cell-free system is indeed recapitulating specific proteomic interactions such as would be observed during *in vitro* fertilization.

Class 2 proteins were identified in the primed control samples but were found in an increased abundance within the cell-free system treated samples. Proteins in this class are expected to be oocyte derived proteins which bind the sperm structures and stay bound. However, this class may also include sperm proteomic changes which are stimulated by the ooplasmic exposure but not directly attributable to oocyte proteins binding the spermatozoa. There is some evidence that during capacitation, nuclear-encoded mRNAs in the spermatozoa are translated by mitochondrial ribosomes, specifically to support capacitation, hyperactivation, acrosomal exocytosis, and fertilization. Mitochondrial proteins, sperm tail axonemal proteins, and acrosomal function related proteins unexpectedly found in this category could be explained by this

theory; this concerns cytochrome C1, cytochrome C oxidase subunit 5A, stomatin like 2, A-kinase anchoring protein 4, NADH:ubiquinone oxidoreductase subunit B5 and B9, and Tektin 1. In fact, STOML2 is a regulator of mitochondrial translation, further providing some credence to this hypothesis. This sperm translation theory remains controversial, however, and does not necessarily explain these trends (Gur & Breitbart, 2006). During Class 2 protein analysis at both time points, we observed an increase in proteasomal subunits/chaperones, as discussed above. Proteins related to spermatogenesis were also identified at each time point. Within Class 2 at both time points, proteins which are known to interact with sperm nuclear DNA during spermatogenesis were identified, including testis-specific serine kinase 6, spermatogenesis associated 24, and PHD finger protein 7. These proteins could perhaps assist in hyper-condensation of the sperm nucleus during spermatogenesis and may also play a role in decondensation of the sperm nucleus upon fertilization. During the 4-hour trial, proteins related to the acrosome reaction, and proteins within the mitochondrial respiratory chain were also identified which is somewhat surprising as we would expect these proteins to begin to be reduced but perhaps this is an indication of some capacitation-like events still taking place early on during our cell-free system co-incubation. Proteins in these categories are no longer identified at 24 hours, perhaps these proteins are early substrates of the ooplasmic protein recycling machinery (**Figure 2C and D**).

Among the Class 3 proteins, those which underwent a reduction in abundance after extract co-incubation, we observed sperm tail, acrosomal, mitochondrial, centrosome-related, spermatogenic, capacitation related, and membrane proteins. These aforementioned structures and systems are no longer necessary after fertilization. Specifically, during the 4-hour trials, 14% of the proteins categorized as Class 3 were tail proteins, 12% were mitochondrial proteins, 6% were spermatogenesis related and 6% were testis/epididymal specific proteins (**Figure 2E**). All of these sperm protein types being degraded during early fertilization would be expected. During the 24-hour trial, 7% of proteins observed were mitochondrial, and 12% were spermatogenesis related, supporting early degradation of some of these substrates. Surprisingly, there were no known tail proteins identified in the 24-hour trial, though 7% of proteins were known structural proteins (**Figure 2F**). Additionally, several autophagy/mitophagy regulators were found within this class as well. Readers will note that during the 4-hour trial, 108 of the 144 proteins identified, or 75%, fell into Class 3. During the 24-hour trial 43 of the 63 identified proteins, or 68%, fell into Class 3. This means that in both trials, the majority of spermatozoa changes observed were reductions in sperm protein content. This is not surprising when considering the context of sperm structure recycling and remodeling during fertilization. Spermatozoa contribute nuclear, chromosomal DNA; a centriole, mRNAs, and a variety of proteins and other molecules to the newly forming embryo; however, the rest of the spermatozoa structures are recycled in an orderly fashion after fertilization (Sutovsky, 2004; Sutovsky & Schatten, 2000). This includes the mitochondrial sheath, as well as structural sperm tail proteins and the remenants of the acrosome, perinuclear theca, and pericentriolar compartment (Sutovsky, 2004). Spermatozoa retain many proteins which ultimately are degraded upon fertilization, a concept which appears to be further reinforced by this study.

Based on this mass spectrometry work, six candidate mitophagy proteins of interest were investigated by using the porcine cell-free system and porcine IVF in conjunction with ICC to detect protein localization patterns within each system. This was done to characterize changes in these proteins during early fertilization events, with an emphasis on exploring their potential roles in post-fertilization mitophagy. We observed that all six proteins appeared to match their mass spectrometry classifications when evaluated by ICC, though PSMG2 and PSMA3 did not increase dramatically in fluorescence intensity (as expected from Class 2 protein), in zygotes, PSMG2 and PSMA3 localization patterns clearly fit the expected increase in abundance. The other 4 proteins corresponded with mass spectrometry results in the cell-free system and in zygotes when observed

via ICC. Additional discussion of these 6 candidate proteins can be found in the Supplemental Discussion section.

In summary, our study harnessed comparative proteomic analysis in conjunction with our novel porcine cell-free system to capture proteomic alterations to spermatozoa which take place during oocyte cytoplasm exposure, a system which has been shown to faithfully mimic some early fertilization events. In total, 185 proteins were identified to undergo significant changes in abundance. Six of these proteins were further investigated and their localization patterns were characterized in the porcine cell-free system and porcine zygotes. These six proteins warrant further exploration but were able to showcase that our mass spectrometry data can be replicated and further understood using immunocytochemistry. More work must be done to further understand these six proteins and more candidates from the 185 proteins inventory should be investigated. However, this mass spectrometry study is the first of its kind to be conducted, and along with the further exploration of six candidates, it highlights the usefulness of our porcine cell-free system for the exploration of early fertilization events, such as post-fertilization sperm mitophagy. This novel system will remain a useful tool to explore early fertilization events at the molecular level.

Materials and Methods

Antibodies and probes

Rabbit polyclonal anti-FUNDC2 (PA570823), MitoTracker® Red CMXRos, and 4',6-diamidino-2-phenylindole (DAPI) were purchased from Invitrogen, Waltham, MA. Mouse monoclonal anti-PSMA3 (BML-PW8115) was purchased from Enzo Life Sciences, Farmingdale, NY. Rabbit polyclonal anti-SAMM50 (20824-I-AP) was purchased from ProteinTech Group, Rosemount, IL. Mouse monoclonal anti-BAG5 (CF810618) was purchased from OriGene Technologies, Rockville, MD. Rabbit polyclonal anti-PACRG (ab4090), rabbit polyclonal anti-SPATA18 (180154), mouse monoclonal anti-MVP (ab14562) and rabbit polyclonal anti-PSMG2 (ab172909) were purchased from Abcam, Cambridge, United Kingdom. HRP-conjugated goat anti-mouse IgG (31430), goat anti-rabbit IgG (31460), goat anti-mouse IgG TRITC (T2762), goat anti-rabbit IgG FITC (65-6111), goat anti-rabbit IgG TRITC (T2769) and goat anti-mouse FITC (62-6511) were purchased from ThermoFischer Scientific, Waltham, MA. Beltsville thawing solution (BTS) boar semen extender supplied with gentamicin was purchased from IMV Technologies, L'Aigle, France. Unless otherwise noted, all chemicals used in this study were purchased from Sigma-Aldrich, St. Lious, MO.

Boar semen collection and processing

Boars were housed at the University of Missouri Animal Science Research Center. Fresh boar semen was collected in one regular collection per week, transferred into 15 mL centrifuge tubes, and centrifuged at 800 × g for 10 min to separate spermatozoa from seminal plasma. Sperm concentration was assessed by using a light microscope and a hemocytometer (ThermoFischer Scientific, Waltham, MA). Only semen collections with >80% motile spermatozoa and <20% morphological abnormalities were used. Spermatozoa were diluted with BTS to a final concentration of 1×10^8 spermatozoa/mL and stored in a sperm incubator at 17°C for up to 5 days.

Collection and in vitro maturation (IVM) of pig oocytes

Porcine ovaries were obtained from a local slaughterhouse. Cumulus-oocyte complexes (COCs) were aspirated from antral follicles of 2-6 mm size and washed three times with HEPES buffered Tyrode Lactate medium containing 0.01% (w/v) polyvinyl alcohol (TL-HEPES-PVA). COCs were transferred into 500 µL wells of oocyte maturation medium (TCM 199, Mediatech, Inc., Manassas, VA) supplemented with 0.1% PVA, 3.05 mM D-glucose, 0.91 mM sodium pyruvate, 20 µg/mL of gentamicin, 0.57 mM cysteine, 0.5 µg/mL LH (L5269), 0.5

µg/mL FSH (F2293), 10 ng/mL epidermal growth factor (E4127), 10% (v/v) porcine follicular fluid. The media was overlaid with mineral oil in four-well dishes (ThermoFischer) and the COCs were incubated at 38.5°C, with 5% CO_2 in the air, for 40 to 44 hours.

In Vitro Fertilization (IVF) and In Vitro Culture (IVC) of Pig Oocytes/Zygotes

Cumulus cells of matured COCs were removed with 0.1% (w/v) hyaluronidase in TL-HEPES-PVA medium. MII oocytes as identified by the presence of a polar body. Mature oocytes were then washed three times with TL-HEPES-PVA medium and once with Tris-buffered medium (mTBM) containing 0.3% (w/v) BSA (A7888). Between 30–40 oocytes were placed into 100 µL drops of the mTBM covered with mineral oil in a 35 mm polystyrene culture dish, then incubated until spermatozoa were prepared for fertilization. Liquid semen preserved in BTS extender solution was washed with PBS containing 0.1% (w/v) PVA (PBS-PVA) two times by centrifugation at 800 x g for 5 min. To stain mitochondria in the sperm tail, the boar spermatozoa were incubated with vital, fixable, mitochondrion-specific probe MitoTracker® Red CMXRos for 10 min at 38.5°C. The spermatozoa pre-labeled with MitoTracker were resuspended in mTBM medium. The sperm suspension in mTBM medium was then added to the 100 µL drops of mTBM medium for a final concentration of 2.5 to 5 x 10^5 spermatozoa/mL. Matured oocytes were incubated with spermatozoa for 5 hours at 38.5°C, with 5% CO_2 in the air, then transferred to 500 µL drops of MU3 medium (Chen et al., 2018) containing 0.4% (w/v) BSA (A6003) for additional culture.

Sperm Priming for Cell-Free System

Boar spermatozoa were washed with phosphate-buffered saline (PBS, 137 mM NaCl, 2.7 mM KCl, 10 mM Na_2HPO_4, 1.8 mM KH_2HPO_4, pH = 7.2) containing 0.1% (w/v) PVA (PBS-PVA) two times by centrifugation at 800 × g for 5 min. The sperm mitochondria were labeled with MitoTracker® Red CMXRos for 10 min at 37°C. At the previously tested concentration of 400 nM, the probe specifically stains boar sperm mitochondria but is also taken up by the sperm head structures (W. H. Song et al., 2016).

To prime sperm mitochondrial sheaths for cell-free studies, spermatozoa pre-labeled with MitoTracker were demembranated/permeabilized with 0.05% (w/v) L-α-lysophosphatidylcholine in KMT (20 mM KCl, 5 mM $MgCl_2$, 50 mM TRIS·HCl, pH = 7.0) for 10 min at 37°C and washed twice with the KMT for 5 min by centrifugation, to terminate the reaction. The spermatozoa were subsequently incubated with 1.0 mM dithiothreitol (DTT) diluted in KMT, pH = 8.2 for 20 min at 37°C and washed twice with KMT for 5 min by centrifugation, to terminate the reaction.

Preparation of Porcine Oocyte Extracts

Cumulus cells of matured COCs were removed with 0.1% (w/v) hyaluronidase in TL-HEPES-PVA medium. The oocytes were then searched for mature MII oocytes as designated by the presence of a polar body. Mature oocytes were then washed three times with TL-HEPES-PVA medium. Zonae pellucidae (ZP) were removed by 0.1% (w/v) pronase (Sigma) in TL-HEPES-PVA. The ZP-free, mature MII oocytes were transferred into an extraction buffer (50 mM KCl, 5 mM $MgCl_2$, 5 mM ethylene glycol-bis[β-aminoethyl ether]-N,N,N',N'-tetraacetic acid [EGTA], 2 mM β-mercaptoethanol, 0.1 mM PMSF, protease inhibitor cocktail [78410, ThermoFischer Scientific], 50 mM HEPES, pH = 7.6) containing an energy-regenerating system (2 mM ATP, 20 mM phosphocreatine, 20 U/mL creatine kinase, and 2 mM GTP), and submerged three times into liquid nitrogen for 5 min each. Next, the frozen-thawed oocytes were crushed by high-speed centrifugation at 16,650 × g for 20 min at 4°C in a Sorvall Biofuge Fresco (Kendro Laboratory Products). Batches of oocyte extract were made from 1,000 oocytes in 100 µL of extract. The supernatants were harvested, transferred into a 1.5 mL tube, and stored in a deep freezer (–80°C).

Co-Incubation of Permeabilized Mammalian Spermatozoa with Porcine Oocyte Extracts

The permeabilized boar spermatozoa were added to porcine oocyte extracts at a concentration of $1x10^4$ spermatozoa/10 µL of an extract and co-incubated for 4–24 h in an incubator at 38.5°C, with 5% CO_2 in the air. After co-incubation, spermatozoa were washed 3x with KMT. At which point the spermatozoa were either processed for immunocytochemistry (as described below), electrophoresis (as described below), or prepared for mass spectrometry analysis (as described below).

Immunocytochemistry

The ICC protocol was performed as described previously (Sutovsky, 2004). Briefly, to fix oocytes or embryos, cells were fixed with 2% (v/v) formaldehyde in PBS for 40 min at room temperature, washed and processed, or stored in PBS at 4°C until used for immunocytochemistry. In some cases, for oocytes and embryos, zona pellucida was removed using 0.1%, (w/v) pronase in TL-HEPES-PVA and the cells were then fixed with 2% (v/v) formaldehyde in PBS for 40 min at room temp. To fix ejaculated, primed, or cell-free treated boar spermatozoa; microscopy coverslips were overlaid with 300 µL of 1% (w/v) aqueous solution of poly-L-lysine, incubated for 5 min, then shaken off, and allowed to dry. The poly-L-lysin coated coverslips were overlaid with 400 µL of warm KMT medium (37°C; pH = 7.3) and 2 µL of sperm suspension (1×10^8 spermatozoa/mL) were added onto coverslips and allowed to settle on the lysine-coated surface for 10 min on a 38.5°C plate. KMT was shaken off from the coverslips and coverslips were overlaid with 2% (v/v) formaldehyde in PBS for 40 min fixation at room temperature, then used for immunocytochemistry immediately or stored at 4°C. Both spermatozoa and oocytes were permeabilized in PBS with 0.1% (v/v) Triton X-100 (PBST) at room temperature for 40 min, then blocked with 5% (v/v) normal goat serum (NGS) in PBST for 25 min. Spermatozoa/oocytes were incubated with the appropriate primary antibodies diluted in PBST containing 1% (v/v) NGS overnight at 4°C. The primary antibodies used throughout the trial and their dilution ratios are as follows: anti-FUNDC2 (1:50), anti-PACRG (1:50), anti-SPATA18 (1:50), anti-MVP (1:50), anti-SAMM50 (1:50), anti-BAG5 (1:50), anti-PSMG2 (1:25) and anti-PSMA3 (1:25). The samples were incubated with appropriate species-specific secondary antibodies such as goat-anti-rabbit (GAR)-IgG-FITC (1:100 dilution), GAR-IgG-TRITC (1:100), goat-anti-mouse (GAM)-IgG-FITC (1:100), or GAM-IgG-TRITC, all diluted 1:100 in PBST with 1% (v/v) NGS for 40 min at room temperature; 2.5 µg/mL DNA stain DAPI was included as well. The samples were mounted on microscopy slides in VectaShield mounting medium (Vector Laboratories, Burlingame, CA), and imaged using a Nikon Eclipse 800 microscope (Nikon Instruments Inc., Melville, NY) with a Retiga QI-R6 camera (Teledyne QImaging, Surrey, BC, Canada) operated by MetaMorph 7.10.2.240. software (Molecular Devices, San Jose, CA). Images were adjusted for contrast and brightness in Adobe Photoshop 2020 (Adobe Systems, Mountain View, CA), to match the fluorescence intensities viewed through the microscope eyepieces.

SDS-PAGE and Western Blotting

The oocyte extracts proteins were prepared for WB by mixing the oocyte extract with 4× LDS loading buffer and ultrapure water to obtain 1× LDS (106 mM Tris·HCl, 141 mM Tris base, 2% (w/v) LDS, 10% (w/v) Glycerol, 0.75% (w/v) Coomassie Blue G250, 0.025% (w/v) Phenol Red, pH = 8.5), supplemented with 2.5% (v/v) β-mercaptoethanol and incubated at 70°C for 10 min prior to use. Spermatozoa were suspended in 1× LDS loading buffer supplemented with 2.5% β-mercaptoethanol. Spermatozoa were incubated at room temperature in 1× LDS loading buffer supplemented with protease inhibitor cocktail for 1 hour on a rocking platform and spun. Total protein equivalent of 50 to 100 million spermatozoa, and 50 MII oocytes were loaded per lane, respectively, on a NuPAGE 4–12% Bis-Tris gel (Invitrogen). Electrophoresis was carried out in the Bis-Tris system using MOPS-SDS running buffer (50 mM MOPS, 50 mM Tris base, 0.1% [w/v] SDS, 1 mM EDTA, pH = 7.7) with the cathode buffer supplemented with 5 mM sodium bisulfite. The molecular masses of separated proteins were

estimated using Novex® Sharp Pre-stained Protein Standard (Invitrogen, LC5800) run in parallel. PAGE was carried out for 5 min at 90 Volts to let the samples delve into the gel and then for another 60–70 min at 200 Volts. The power was limited to 20 Watts. After PAGE, proteins were electro-transferred to polyvinylidene fluoride (PVDF) membranes (MilliporeSigma, Burlington, MA) using Owl wet transfer system (ThermoFischer Scientific) at 65 Volts for 90 min for immunodetection, using Bis-Tris-Bicine transfer buffer (25 mM Bis-Tris base, 25 mM Bicine, 1 mM EDTA, pH = 7.2) supplemented with 10% (v/v) methanol per membrane, and 2.5 mM sodium bisulfite. The membranes with the transferred proteins were blocked with 10% (w/v) non-fat milk in TBS with 0.05% (v/v) Tween 20 (TBST, Sigma) for 40 min. The membranes were then incubated with the appropriate primary antibodies diluted in 5% non-fat milk in TBST overnight at 4°C. The primary antibodies used throughout the trial and their dilution ratios are as follows: anti-FUNDC2 (1:1000), anti-PACRG (1:1000), anti-SPATA18 (1:1000), anti-MVP (1:1000), anti-SAMM50 (1:1000), anti-BAG5 (1:1000), anti-PSMG2 (1:1000) and anti-PSMA3 (1:1000). The membranes were subsequently incubated with appropriate species-specific secondary antibodies such as HRP-conjugated goat anti-mouse IgG (GAM-IgG-HRP), or goat anti-rabbit (GAR-IgG-HRP) for 40 min at room temperature. The membranes were reacted with chemiluminescent substrate (Millipore), detected using ChemiDoc Touch Imaging System (Bio-Rad, Hercules, CA, USA) to record the protein bands, and analyzed by Image Lab Software (ver. 5.2.1, Bio-Rad, Hercules, CA, USA). The membranes were stained with CBB R-250 after chemiluminescence detection for protein load control.

Mass Spectrometry Sample Preparation

Cell-free system exposed spermatozoa, spermatozoa controls, and oocyte extract underwent protein precipitation using a TCA protein precipitation protocol from Dr. Luis Sanchez. These samples were then resuspended in acetone and submitted to the University of Missouri Gehrke Proteomics Center for MALDI-TOF Mass Spectrometry analysis. At the Proteomics Center, these samples were washed by 80% cold acetone twice. Then 10 µl 6M urea 2M thiourea and 100mM ammonium bicarbonate was added to the protein pellet. Solubilized protein was reduced by DTT and alkylated by iodoacetamide. Then trypsin was added for disgestion overnight. The digested peptides were C18 ziptip deslated, lyophilized and resuspended in 10 µL 5/0.1% acetonitrile/formic acid.

A volume of 1 µL of suspended peptides was loaded onto a C18 column with a step gradient of acetonitrile at 300 nL/min. A Bruker nanoElute system was connected to a timsTOF pro mass spectrometer. The loaded peptide was eluted at a flow rate of 300 nl/min with the initial gradient of 3% B (A: 0.1% formic acid in water, B: 99.9% acetonitrile, 0.1% formic acid), followed by 11 min ramp to 17%B, 17-25% B over 21 min, 25-37% B over 10 min, 37-80% B over 4 min, holding at 80% B for 9 min, 80-3% B in 1 min, and holding at 3% B for 3 min. Total running time was 60 min.

Raw data was searched using PEAKs (version X+) with UniProt *Sus scrofa* protein database downloaded March 01, 2019 with 88374 itmes. Samples were searched with trypsin as enzyme, 4 missed cleavages allowed; carbamidomethyl cysteine as a fixed modification; oxidized methionine and acetylation on protein N terminus as variable modification. 50 ppm mass tolerance on precursor ions, 0.1Da on fragment ions. For the protein identification, the following criteria were used: peptide FDR and protein FDR < 1%, and >=4 spectrum per protein in each sample. Samples were submitted in triplicate for both the 4- and 24-hours cell-free system trials.

Mass Spectrometry Data Statistical Analysis

Prior to statistical analysis, the primed and cell-free treated sperm samples were normalized based on the content of outer dense fiber proteins (ODF) 1, 2, and 3. To further reduce batch variance, the protein spectrum counts were also subject to normalization by means. After these normalization steps, the primed

and cell-free extract treated sperm samples were statistically compared using a paired T-test. This T-test was comparing the relative normalized protein abundance between our primed control and cell-free treated samples. *P*<0.1 and *P*<0.2 was considered to indicate statistical significance.

Protein Classification

Both the 4-hour and 24-hour protein inventories were divided into three different classes. Class 1 proteins were detected only in the oocyte extract (not in the vehicle control or primed control spermatozoa) and found on the spermatozoa only after extract co-incubation. These proteins are interpreted as ooplasmic mitophagy receptors/determinants and nuclear/centrosomal remodeling factors (p<0.2). Class 2 proteins were detected in the primed spermatozoa but increased in the spermatozoa exposed to cell-free system co-incubation (p<0.1). Class 3 proteins were present in both the gametes or only the spermatozoa, but are decreased in the spermatozoa after co-incubation, interpreted as sperm-borne mitophagy determinants and/or sperm-borne proteolytic substrates of the oocyte autophagic system (p<0.1).

Functional analysis

Following the statistical analysis and protein classification, the function of all proteins p<0.1 (p<0.2 for Class 1), were searched using a PubMed literature search and UniProt Knowledgebase search. Known functions can be found in **Table 1** and **Table 2**. Proteins were then categorized based on known functions and known roles within pathways, in gametes and/or somatic cells. Protein categorization results can be found in the pie chart images of **Figure 2**.

Acknowledgements

We are truly thankful for the support received from the staff of the National Swine Research and Resource Center, the University of Missouri, funded by National Institutes of Health (NIH) grant U42 OD011140, as well as Professor Randall Prather and his associates for their kind support, including but not limited to gilt ovary and boar semen collections. We would also like to thank the University of Missouri Gehrke Proteomics Center, and their staff who conducted the mass spectrometry data collection and statistical analysis.

References

Al Rawi, S., Louvet-Vallee, S., Djeddi, A., Sachse, M., Culetto, E., Hajjar, C., . . . Galy, V. (2011). Postfertilization autophagy of sperm organelles prevents paternal mitochondrial DNA transmission. *Science, 334*(6059), 1144-1147. doi:10.1126/science.1211878

Anderson, S., Bankier, A. T., Barrell, B. G., de Bruijn, M. H., Coulson, A. R., Drouin, J., . . . Young, I. G. (1981). Sequence and organization of the human mitochondrial genome. *Nature, 290*(5806), 457-465. doi:10.1038/290457a0

Ankel-Simons, F., & Cummins, J. M. (1996). Misconceptions about mitochondria and mammalian fertilization: implications for theories on human evolution. *Proc Natl Acad Sci U S A, 93*(24), 13859-13863. doi:10.1073/pnas.93.24.13859

Baker, M. A., Reeves, G., Hetherington, L., Müller, J., Baur, I., & Aitken, R. J. (2007). Identification of gene products present in Triton X-100 soluble and insoluble fractions of human spermatozoa lysates using LC-MS/MS analysis. *Proteomics Clin Appl, 1*(5), 524-532. doi:10.1002/prca.200601013

Chen, P. R., Redel, B. K., Spate, L. D., Ji, T., Salazar, S. R., & Prather, R. S. (2018). Glutamine supplementation enhances development of in vitro-produced porcine embryos and increases leucine consumption from the medium. *Biol Reprod, 99*(5), 938-948. doi:10.1093/biolre/ioy129

Gur, Y., & Breitbart, H. (2006). Mammalian sperm translate nuclear-encoded proteins by mitochondrial-type ribosomes. *Genes & Development, 20*(4), 411-416. doi:10.1101/gad.367606

Hajnóczky, G., Csordás, G., Das, S., Garcia-Perez, C., Saotome, M., Sinha Roy, S., & Yi, M. (2006). Mitochondrial calcium signalling and cell death: approaches for assessing the role of mitochondrial Ca2+ uptake in apoptosis. *Cell Calcium, 40*(5-6), 553-560. doi:10.1016/j.ceca.2006.08.016

Kaneda, H., Hayashi, J., Takahama, S., Taya, C., Lindahl, K. F., & Yonekawa, H. (1995). Elimination of paternal mitochondrial DNA in intraspecific crosses during early mouse embryogenesis. *Proc Natl Acad Sci U S A, 92*(10), 4542-4546. doi:10.1073/pnas.92.10.4542

Liau, W. S., Gonzalez-Serricchio, A. S., Deshommes, C., Chin, K., & LaMunyon, C. W. (2007). A persistent mitochondrial deletion reduces fitness and sperm performance in heteroplasmic populations of C. elegans. *BMC Genet, 8*, 8. doi:10.1186/1471-2156-8-8

Luo, S., Valencia, C. A., Zhang, J., Lee, N. C., Slone, J., Gui, B., . . . Huang, T. (2018). Biparental Inheritance of Mitochondrial DNA in Humans. *Proc Natl Acad Sci U S A, 115*(51), 13039-13044. doi:10.1073/pnas.1810946115

Martínez-Heredia, J., Estanyol, J. M., Ballescà, J. L., & Oliva, R. (2006). Proteomic identification of human sperm proteins. *Proteomics, 6*(15), 4356-4369. doi:10.1002/pmic.200600094

McBride, H. M., Neuspiel, M., & Wasiak, S. (2006). Mitochondria: more than just a powerhouse. *Curr Biol, 16*(14), R551-560. doi:10.1016/j.cub.2006.06.054

McFarland, R., Taylor, R. W., & Turnbull, D. M. (2007). Mitochondrial disease--its impact, etiology, and pathology. *Curr Top Dev Biol, 77*, 113-155. doi:10.1016/S0070-2153(06)77005-3

Miyamoto, K., Furusawa, T., Ohnuki, M., Goel, S., Tokunaga, T., Minami, N., . . . Imai, H. (2007). Reprogramming events of mammalian somatic cells induced by Xenopus laevis egg extracts. *Mol Reprod Dev, 74*(10), 1268-1277. doi:10.1002/mrd.20691

Miyamoto, K., Tsukiyama, T., Yang, Y., Li, N., Minami, N., Yamada, M., & Imai, H. (2009). Cell-free extracts from mammalian oocytes partially induce nuclear reprogramming in somatic cells. *Biol Reprod, 80*(5), 935-943. doi:10.1095/biolreprod.108.073676

Pilatz, A., Lochnit, G., Karnati, S., Paradowska-Dogan, A., Lang, T., Schultheiss, D., . . . Wagenlehner, F. (2014). Acute epididymitis induces alterations in sperm protein composition. *Fertil Steril, 101*(6), 1609-1617.e1601-1605. doi:10.1016/j.fertnstert.2014.03.011

Politi, Y., Gal, L., Kalifa, Y., Ravid, L., Elazar, Z., & Arama, E. (2014). Paternal mitochondrial destruction after fertilization is mediated by a common endocytic and autophagic pathway in Drosophila. *Dev Cell, 29*(3), 305-320. doi:10.1016/j.devcel.2014.04.005

Sato, M., & Sato, K. (2011). Degradation of paternal mitochondria by fertilization-triggered autophagy in C. elegans embryos. *Science, 334*(6059), 1141-1144. doi:10.1126/science.1210333

Schwartz, M., & Vissing, J. (2002). Paternal inheritance of mitochondrial DNA. *N Engl J Med, 347*(8), 576-580. doi:10.1056/NEJMoa020350

Sharpley, M. S., Marciniak, C., Eckel-Mahan, K., McManus, M., Crimi, M., Waymire, K., . . . Wallace, D. C. (2012). Heteroplasmy of mouse mtDNA is genetically unstable and results in altered behavior and cognition. *Cell, 151*(2), 333-343. doi:10.1016/j.cell.2012.09.004

Shitara, H., Hayashi, J. I., Takahama, S., Kaneda, H., & Yonekawa, H. (1998). Maternal inheritance of mouse mtDNA in interspecific hybrids: segregation of the leaked paternal mtDNA followed by the prevention of subsequent paternal leakage. *Genetics, 148*(2), 851-857.

Slone, J., Zou, W., Luo, S., Schmitt, E. S., Chen, S. M., Wang, X., . . . Huang, T. (2020). doi:10.1101/2020.02.26.939405

Song, W.-H., Zuidema, D., Yi, Y.-J., Zigo, M., Zhang, Z., Sutovsky, M., & Sutovsky, P. (2021). Mammalian Cell-Free System Recapitulates the Early Events of Post-Fertilization Sperm Mitophagy. *Cells, 10*(9), 2450. doi:10.3390/cells10092450

Song, W. H., & Sutovsky, P. (2018). Porcine Cell-Free System to Study Mammalian Sperm Mitophagy. *Methods Mol Biol*. doi:10.1007/7651_2018_158

Song, W. H., Yi, Y. J., Sutovsky, M., Meyers, S., & Sutovsky, P. (2016). Autophagy and ubiquitin-proteasome system contribute to sperm mitophagy after mammalian fertilization. *Proc Natl Acad Sci U S A, 113*(36), E5261-5270. doi:10.1073/pnas.1605844113

Sutovsky, P. (2004). Visualization of sperm accessory structures in the mammalian spermatids, spermatozoa, and zygotes by immunofluorescence, confocal, and immunoelectron microscopy. *Methods Mol Biol, 253*, 59-77. doi:10.1385/1-59259-744-0:059

Sutovsky, P. (2011). Sperm proteasome and fertilization. *Reproduction, 142*(1), 1-14. doi:10.1530/REP-11-0041

Sutovsky, P., Manandhar, G., Laurincik, J., Letko, J., Caamano, J. N., Day, B. N., . . . Sutovsky, M. (2005). Expression and proteasomal degradation of the major vault protein (MVP) in mammalian oocytes and zygotes. *Reproduction, 129*(3), 269-282. doi:10.1530/rep.1.00291

Sutovsky, P., McCauley, T. C., Sutovsky, M., & Day, B. N. (2003). Early degradation of paternal mitochondria in domestic pig (Sus scrofa) is prevented by selective proteasomal inhibitors lactacystin and MG132. *Biol Reprod, 68*(5), 1793-1800. doi:10.1095/biolreprod.102.012799

Sutovsky, P., Moreno, R. D., Ramalho-Santos, J., Dominko, T., Simerly, C., & Schatten, G. (1999). Ubiquitin tag for sperm mitochondria. *Nature, 402*(6760), 371-372. doi:10.1038/46466

Sutovsky, P., Moreno, R. D., Ramalho-Santos, J., Dominko, T., Simerly, C., & Schatten, G. (1999). Ubiquitin tag for sperm mitochondria. *Nature, 402*(6760), 371-372. doi:10.1038/46466

Sutovsky, P., & Schatten, G. (2000). Paternal contributions to the mammalian zygote: fertilization after sperm-egg fusion. *Int Rev Cytol, 195*, 1-65. Retrieved from https://www.ncbi.nlm.nih.gov/pubmed/10603574

Sutovsky, P., Simerly, C., Hewitson, L., & Schatten, G. (1998). Assembly of nuclear pore complexes and annulate lamellae promotes normal pronuclear development in fertilized mammalian oocytes. *J Cell Sci, 111 (Pt 19)*, 2841-2854. Retrieved from https://www.ncbi.nlm.nih.gov/pubmed/9730977

Sutovsky, P., Van Leyen, K., McCauley, T., Day, B. N., & Sutovsky, M. (2004). Degradation of paternal mitochondria after fertilization: implications for heteroplasmy, assisted reproductive technologies and mtDNA inheritance. *Reprod Biomed Online, 8*(1), 24-33. Retrieved from https://www.ncbi.nlm.nih.gov/pubmed/14759284

Zhang, M., Chiozzi, R. Z., Skerrett-Byrne, D. A., Veenendaal, T., Klumperman, J., Heck, A. J. R., . . . Bromfield, E. G. (2022). High Resolution Proteomic Analysis of Subcellular Fractionated Boar Spermatozoa Provides Comprehensive Insights Into Perinuclear Theca-Residing Proteins. *Front Cell Dev Biol, 10*, 836208. doi:10.3389/fcell.2022.836208

Zhou, Q., Li, H., & Xue, D. (2011). Elimination of paternal mitochondria through the lysosomal degradation pathway in C. elegans. *Cell Res, 21*(12), 1662-1669. doi:10.1038/cr.2011.182

Zigo, M., Manaskova-Postlerova, P., Jonakova, V., Kerns, K., & Sutovsky, P. (2019). Compartmentalization of the proteasome-interacting proteins during sperm capacitation. *Scientific Reports, 9*(1). doi:10.1038/s41598-019-49024-0

Zimmerman, S. W., Manandhar, G., Yi, Y. J., Gupta, S. K., Sutovsky, M., Odhiambo, J. F., . . . Sutovsky, P. (2011). Sperm proteasomes degrade sperm receptor on the egg zona pellucida during mammalian fertilization. *PLoS One, 6*(2), e17256. doi:10.1371/journal.pone.0017256

Zuidema, D., & Sutovsky, P. (2019). The domestic pig as a model for the study of mitochondrial inheritance. *Cell Tissue Res*. doi:10.1007/s00441-019-03100-z